FCTUC DEPARTAMENTO DE ENGENHARIA CIVIL
FACULDADE DE CIÊNCIAS E TECNOLOGIA
UNIVERSIDADE DE COIMBRA

"Hybrid Lattice-Tubular steel wind towers: Conceptual design of tower"

Dissertação apresentada para a obtenção do grau de Mestre em Engenharia Civil na Especialidade de Mecânica Estrutural

Autor
João Rafael Branquinho Maximino

Orientador
Carlos Alberto da Silva Rebelo
Milan Veljkovic

Esta dissertação é da exclusiva responsabilidade do seu autor, não tendo sofrido correcções após a defesa em provas públicas. O Departamento de Engenharia Civil da FCTUC declina qualquer responsabilidade pelo uso da informação apresentada

Coimbra, Julho, 2015

AGRADECIMENTOS

Agradeço em primeiro lugar aos meus pais, por todo o apoio demonstrado ao longo dos anos, e pelos ensinamentos fundamentais que me levaram a este momento. Ao meu irmão, que sempre esteve ao meu lado, obrigado pela motivação em todos os momentos. A toda a minha família pela união, apoio, coragem e vontade que sempre me transmitiram. À minha namorada, que desde o início tornou esta experiência melhor para mim, e me ajudou a crescer como pessoa.

Aos meus colegas que me acompanharam e apoiaram neste percurso, a todos os professores que me transmitiram tudo o que aprendi até agora, o meu muito obrigado.

Por fim gostaria de agradecer à Universidade Técnica de Lulea por me ter acolhido na realização desta tese de mestrado, e mostrar a minha gratidão ao Professor Doutor Carlos Alberto da Silva Rebelo e ao Professor Doutor Milan Veljkovic pela orientação e disponibilidade dispensada.

ABSTRACT

The utilization of the wind is not a new technology, but an evolution of old processes and techniques. Like nowadays, wind power had a huge role in the past, with different utilizations and proposes, although the main goal was always to help in the Human's heavy work. The distribution of cheap coal and oil fuels brought an era where wind energy had to fight to keep itself alive, only resisting in some irrelevant niches. Today, as the coal, oil and nuclear energy are facing an increasing resistance, the re-emerged wind power is an inevitable solution.

The main objective for this thesis is to develop and optimize a new hybrid steel solution for supporting a multi-megawatt wind turbine, composed by a lower steel lattice structure, supporting a steel tubular upper part. The solution is targeted at tall onshore applications. In the study performed, a new cross section will be used, in order to be possible to assemble the lattice part only with bolted connections, making it a quicker process and more efficient when subjected to fatigue loads.

The lattice part introduces the possibility to increase the total high of the tower without having the problems with the transportation of the structure for the assembly place, what would not be possible using only the steel tubular part, which is the most common use nowadays. For the optimization of this part of the structure, parametrical study of the design of the structure, with special focus on the number of supports and on the cross section of the bars, using a circular hollow section for the elements, with special attention on the global and local stability of the elements.

RESUMO

A utilização da energia eólica não é uma nova tecnologia, mas sim uma evolução de processos e técnicas antigas. Como nos dias de hoje, a energia eólica teve um grande papel no passado, com diferentes utilizações e propósitos, embora o principal objetivo tenha sido o de facilitar os trabalhos mais pesados para o ser humano. A distribuição fácil de carvão e petróleo trouxeram uma era nova era onde a energia eólica teve que lutar para manter-se no mercado, apenas resistindo em alguns nichos financeiros, embora irrelevantes. Nos dias de hoje, com o carvão, petróleo e energia nuclear a enfrentar uma resistência cada vez maior, a energia eólica passou a ser uma solução inevitável para o problema.

Assim, o principal propósito desta tese é desenvolver e otimizar uma nova solução híbrida de aço para suporte de uma turbina eólica multi-megawatt, composta por uma estrutura em treliça para a base, servindo de apoio a uma parte de aço tubular. A solução é destinada a aplicação *onshore*, para estruturas com alturas relevantes. No estudo levado a cabo, irá ser utilizado um novo tipo de secções transversais, com o intuito de permitir a montagem da estrutura apenas com ligações aparafusadas, tornando assim a montagem num processo mais rápido, e a estrutura mais eficiente quando sujeita a cargas de fadiga.

A parte inferior introduz a possibilidade de aumentar a altura total da torre, sem ter os problemas com o transporte da estrutura ou da montagem no local, o que não seria possível utilizando apenas a parte tubular, a mais comum das utilizações. Para a otimização desta parte da estrutura, vai ser efetuado um estudo paramétrico entre várias geometrias, número de suportes e secção transversal das secções, utilizando secções circulares ocas para os elementos, com principal foco na estabilidade global e estabilidade local dos elementos.

TABLE OF CONTENTS

TABLE OF FIGURES

1 INTRODUCTION

1.1 Wind Energy

Global warming has become the most talked environmental issue of today's life. Once it became a priority issue, governments, corporations, and individual all around the world are debating the best and possible solutions for this problem. The development of renewable energy technologies are one of the most potential solution for this problem, which are global challenging issues. Renewable energy is the energy that rely on fuel sources that restore themselves over short periods of time and do not diminish, such as the wind, sun, moving water, the earth's heat (geothermal) and waste material (biomass).

1.1.1 Wind Energy in Europe

Nowadays, the wind energy is facing a huge development, not only in the increasing technology, but also in the amount of annual installed wind capacity. Annual installations of wind power have increased over the past 14 years, from 3.2 GW in 2000, to 11.5 GW in 2014, at an annual growth of 9.8%. As we can see in the Figure 1-1, a total of 128.8 GW is now installed in the European Union.
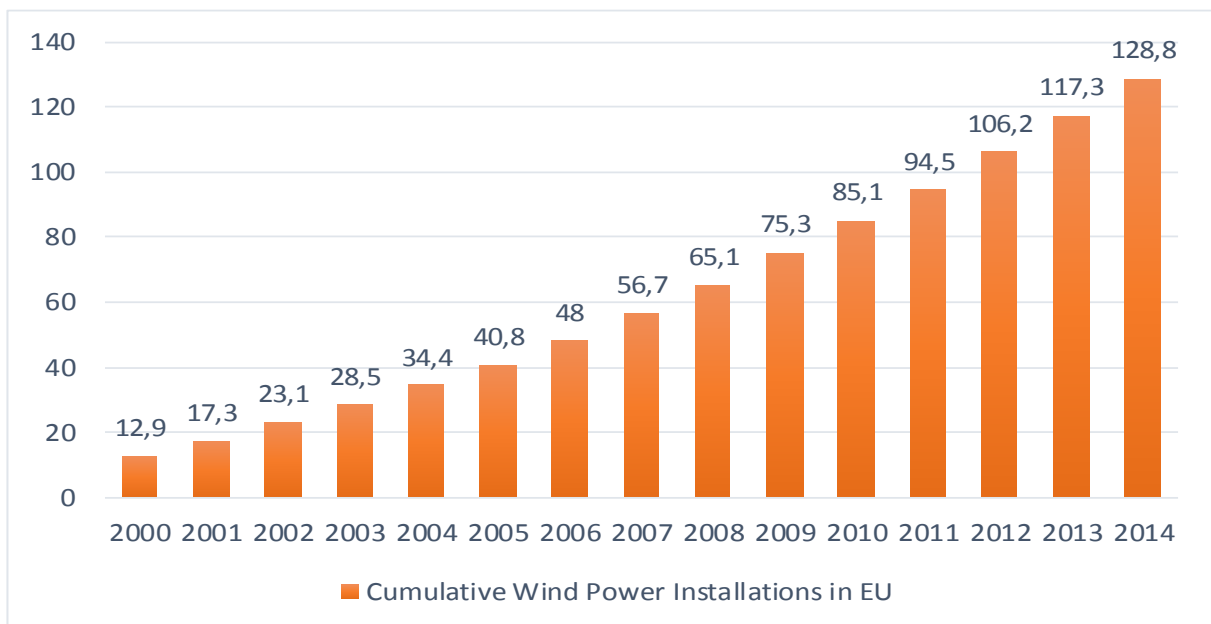
Figure 1-1 - Cumulative Wind Power Installation in EU

In all the Europe an effort has been made in order to achieve a higher percentage of energy produced by renewable sources. In the last year, 79.1% of new power capacity installations, which corresponds 21.3 GW, were from renewable sources. Since the new millennium, renewable capacity increased from 24.4% of total power capacity to 41.5% in 2014, with the

wind energy worth 14.1% in 2014 when in the year of 2000 it only produces 2.4% as we can see on Figure 1-2.
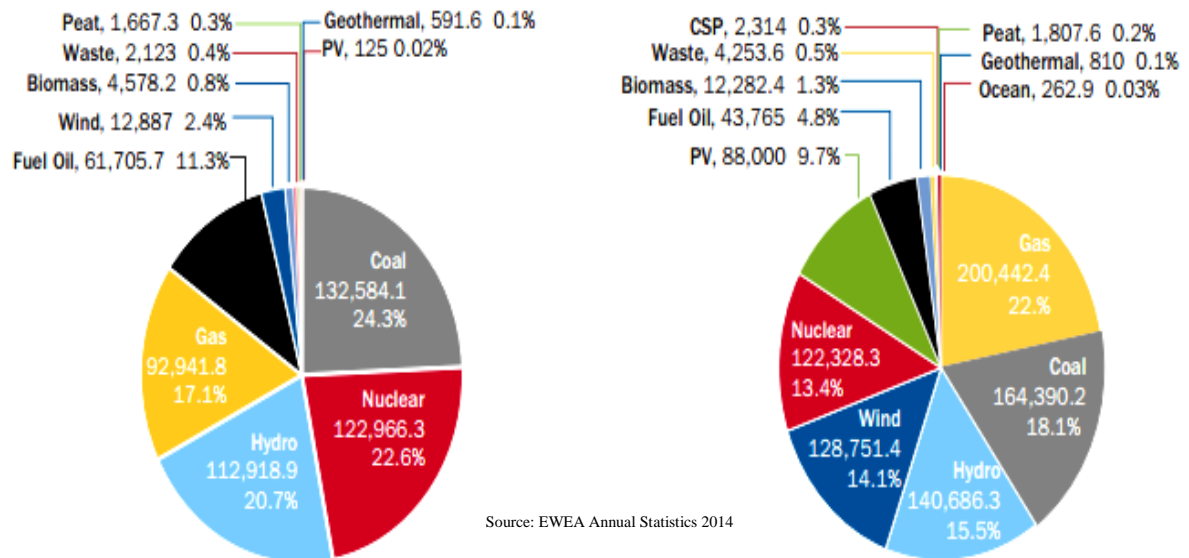
Source: EWEA Annual Statistics 2014

Figure 1-2 - Comparison of EU power mix in the year of 2000 (left) and 2014 (right)

Germany remains the EU country with the largest installed capacity, followed by Spain, the UK, France and Italy. Ten other EU countries have over than 1 GW of installed capacity, such as Austria, Belgium, Greece, Ireland, the Netherlands, Poland, Romania, Denmark, Portugal and Sweden, with the last three having more than 4 GW of installed wind energy capacity. The wind energy capacity currently installed in the EU would be able to produce in an average wind year 284 TWh of electricity, the amount to cover 10.2% of the EU's total consumption.
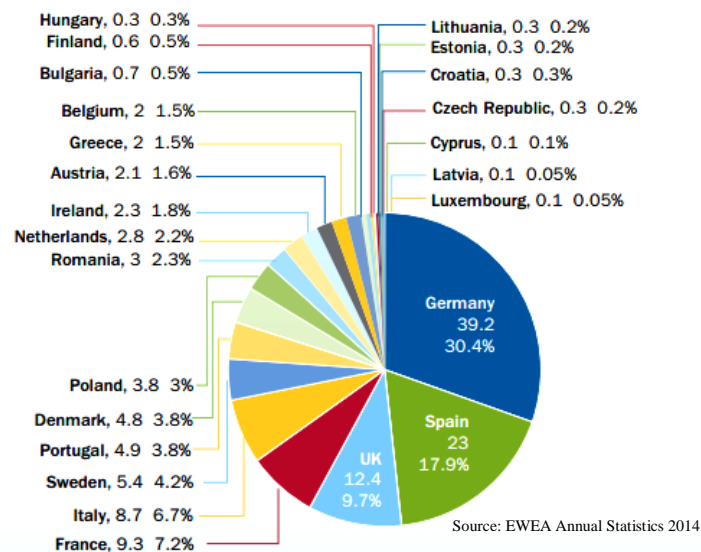
Source: EWEA Annual Statistics 2014

Figura 1-3 - EU Member State market shares for total installed capacity

1.1.2 Wind Energy of the world

Across the world, many countries are installing a large quantity of wind turbines in order to achieve a higher percentage of electricity produced by this type of source. From the last 15 years, the global wind capacity installed is getting bigger each year, who shows the importance that this kind of energy type is having for all the countries. Popular Republic of China, Germany and USA, were the countries that got most installed capacity in the year of 2014. They are also the ones with higher cumulative capacity by December of the same year.

TOP 10 NEW INSTALLED CAPACITY JAN-DEC 2014

Country	MW	% SHARE
PR China*	23,351	45.2
Germany	5,279	10.2
USA	4,854	9.4
Brazil**	2,472	4.8
India	2,315	4.5
Canada	1,871	3.6
United Kingdom	1,736	3.4
Sweden	1,050	2.0
France	1,042	2.0
Turkey	804	1.6
Rest of the world	6,702	13.0
Total TOP 10	**44,775**	**87**
World Total	**51,477**	**100**

Source: GWEC

TOP 10 CUMULATIVE CAPACITY DEC 2014

Country	MW	% SHARE
PR China*	114,763	31.0
USA	65,879	17.8
Germany	39,165	10.6
Spain	22,987	6.2
India	22,465	6.1
United Kingdom	12,440	3.4
Canada	9,694	2.6
France	9,285	2.5
Italy	8,663	2.3
Brazil**	5,939	1.6
Rest of the world	58,275	15.8
Total TOP 10	**311,279**	**84.2**
World Total	**369,553**	**100**

Source: GWEC

Figure 1-4 - Global TOP 10 of new installed (left) and cumulative capacity (right)

By that, new technologies and new ways of construction have to be investigated, in order to get the maximum of this resource. With the increase of the capacity of the turbines, from 0.5 MW to around 7 MW, although turbines between the 2 and 5 MW of capacity are the most popular and common, the wind towers need to increase the structural strength and the stiffness that is required to support such turbines.

According to (Hau, 2013), the transportation and the erection procedure is developing into an increase problem for the last generation of multi-megawatt wind turbines. With heights of more than 100 meters, the required diameter at the tower base is more than 5 meters, which are not able to the road transportation. This problem becomes a strong incentive to find innovative solutions in the tower design, for the wind energy continues to maintain the competitiveness in the future.

1.2 China: The Good, the Bad and the Ugly

China in the largest consumer and producer of coal in the world, and is the biggest user of coal-derived electricity, around 79% of the 5 649 500 GWh that are produced by year, to supply the enormous electricity consumption. The remainder percentage is completed by 1.8% of natural gas, 0.2% of oil, 14.8% are produced in Hydro power facilities, 2.2% from another renewable energies, 1.8% from nuclear power and 0.2% derivate from other sources. With the comparison of the percentages, is easy to conclude about the dependence of coal from China.
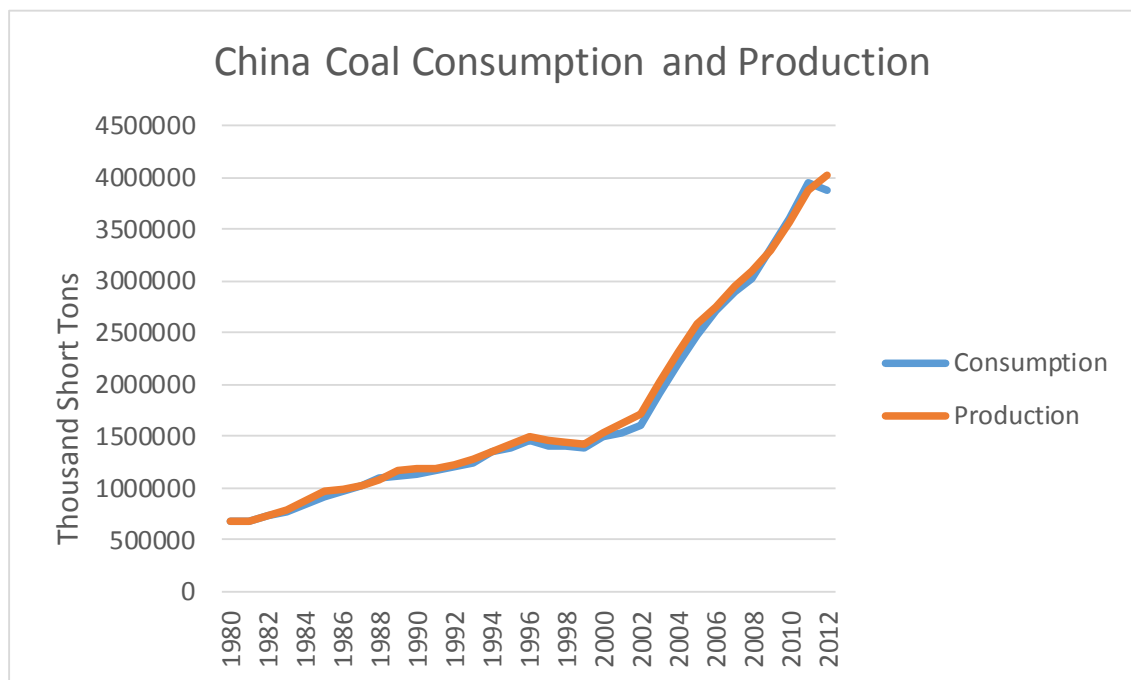
Figure 1-5 - Coal Production vs Consumption (EIA)

Comparing the types of new installed energy in the year of 2014, it's possible to see that this kind of energy production and the dependence of the coal will not going to change in the future years. Despite the addition of substantial wind, solar and nuclear power plants capacity, when adjusted for the amount of annual energy produced per unit of capacity, the amount of new coal energy added to China grid of electricity last year exceeded solar energy by 17 times, wind energy by more than 4 times and Hydropower for more than 3 times.
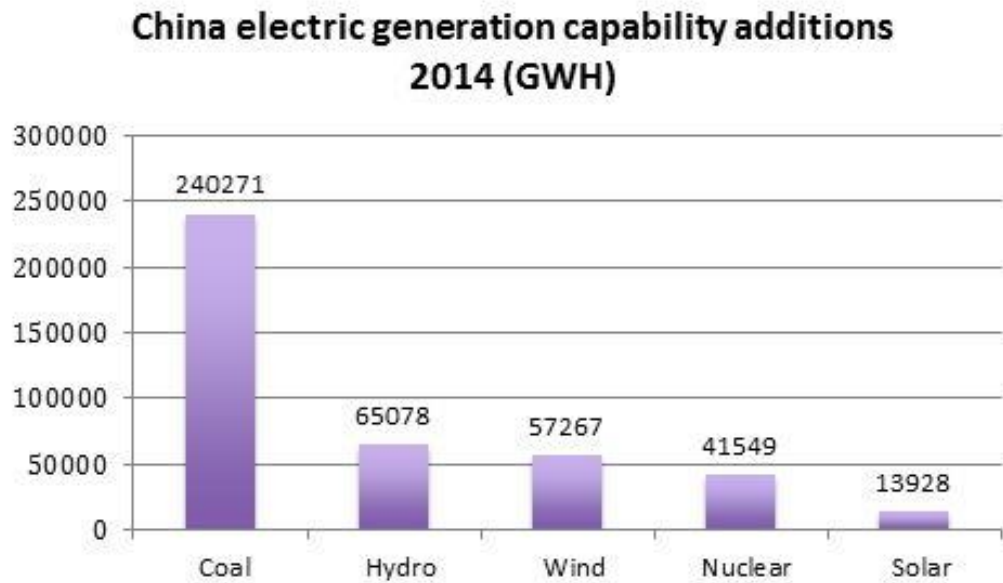
Figure 1-6 - New installed capacity in 2014 (Clean Air Task Force, 2015)

This amount of coal power plants help to explain the fact that China is the country in the world with major effect in air pollution and emission of CO_2. It is now the number one producer of carbon dioxide, and responsible for 25% of the world's output. According to a recent study, even if the USA emissions were to suddenly disappear, the total emissions would be back at the same values in a space of four years, as a result of China's growth alone. (Moller, Elisabeth (2013), The Telegraph).

With the projections pointing in an energy consumption growth of 60% until 2035, and the production increasing 45%, China will become the largest energy importer. With this increase of production, is expected that the CO_2 emissions to increase by 37% and China alone will be responsible for 1/3 of the global emissions. In order to improve the air quality in China's greatest cities, the government is considering to move the last four coal-fired power plants out of Beijing's municipal area, and replacing them with gas-fired stations, that are much cleaner, and make possible to improve the quality of the air in the city, which nowadays is causing an alarming number of fatalities.

Figure 1-7 - Beijing's Smog (Reuters)

Although the coal power plants are the most used electricity production type, for the past few years China is leading the world's statistics in new and cumulative wind power installed capacity. Since five years ago, the cumulative installed capacity has increased more than 4 times, from 25805 MW installed in 2009 to 114609 MW in 2014, as demonstrated on Figure 1-8 being the first country to overcome the 100GW mark, which represents 31% of the global capacity. The year of 2014 could also be marked as the first time a single country installed over 20 GW, with a new installed capacity of 23351 MW. Even with the increase of installed power, the total production only supplies 2.78% of the national electricity consumption.
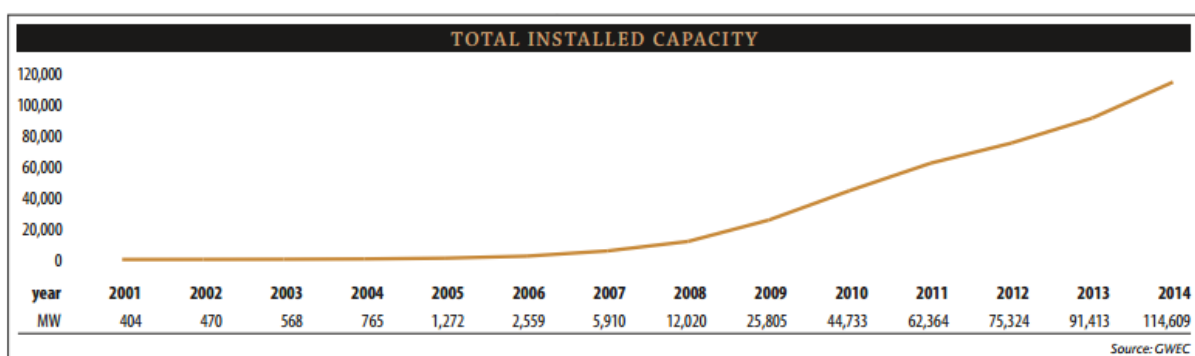
Figure 1-8 - China's Total Installed Capacity since 2001 (GWEC)

One of the biggest problems for the growth of the installed values and the exploitation of the total installed is the grid connection system. With the fast development of wind power in China, the country's electricity grid infrastructure is not prepared for the amount of energy being produced and is under an enormous strain, with some projects stopped for several months until they are connected to the national grid. In 2010, an agreement was made with the

Chinese operator State Grid, in order to connect 100 GW of wind power by the year of 2015, but according to the 2014 GWEC report, these values where not achieved as supposed, and the current situation is not likely to change in the near future, in the terms of a new and more capable grid being installed.

Notwithstanding the difficulties talked before, the future of the wind power in China seems to be secured, as the government has proposed a low-carbon strategy, with the wind power to be one of the main technologies to achieve such targets. According to China Wind Roadmap from 2012, is expected that the total installed capacity in 2020, 2030, and 2050 to be 200 GW, 400 GW and 1000 GW, respectively, and meet 17% of the electricity demand. As technologies improves, this objectives seem easy to reach. In order to accomplish the objectives above, the investment in wind power is estimated to be around CNT 12000 billion, close to 2000 Million €. Whit this investment, is expected that around the year of 2020, the cost of wind power energy to be the same or close to the cost of coal power. The social and environmental benefits will also be considerable, with an estimated 720000 jobs to be created and the emissions of $CO2$ would be much smaller when compared to the present day.

Figure 1-9 - Gansu Wind Farm in China (goldpower.net)

For all the objectives be fulfilled, not only in China but in the whole world, wind energy sector players, such as universities, wind power research institutes, wind turbines manufacturers and many other companies and intervenient, need to prepare the future, making the wind energy more competitive and promoting the application, investing sufficient money and working together in order to encourage large-scale wind power facilities around the world.

1.3 Summary

This thesis is composed in 7 chapters:

Chapter 1 – Introduction
Chapter 2 – State of Art
Chapter 3 – Background Theory
Chapter 4 – Conceptual Model and Design of the Lattice Tower
Chapter 5 – Cross Section – Properties and Design
Chapter 6 – Connection Study and Design
Chapter 7 – Conclusions

2 STATE OF ART

We cannot know to where we are going, if we don´t perceive from where we've come. So, when discussing and investigating wind towers and wind turbines, knowing the historical roots of wind power technology is an absolute need, because the multiple successes and failures of the past will provide hints and clues for the future development. With this, the following state of art starts with a background on the origin for the use of the wind, in order to understand the present use for this resource.

2.1 *The origins of windmills*

There are not a convincing proof about the historical origins of windmills, but some authors maintain that remains of stone windmills were found in Egypt, near Alexandria, with an estimated age of 3000 years. However, there are no certainties that the old empires such Greeks or Romans really knew and used windmills. The first reliable information dates form 644 Anno Domini, and a later description of the year of 945, and describes a vertical axis windmill, see Figure 2-1, used for milling grain, from the Persian-Afghan border. Some centuries later, the Chinese were also using windmills to drains rice fields, but it´s not possible to determine the year in which they started to use the wind as a power source to their activities.

Figure 2-1 - Afghan Windmill with vertical axis (oratoryorphanage.org)

The more traditional windmill with a horizontal axis was invented in Europe, independently of the existing vertical axis of rotation. The first information has its origin in 1180 in the Duchy of Normandy, which quickly spread to the North and East of Europe. In Germany,

numerous post windmills could be found in the 13th century. In Holland, several improvements were made in the 16th century, leading to a new type of mil called "Dutch Windmill". In this type of mills, the capacity of the tower cap to turn with the wind wheel, permitted an increase of the applications for this type of structure. In addition to the post windmills that were entirely made of wood, in the Mediterranean region, a traditional type of windmill, the so-called "Tower Windmills" make their appearance one or two centuries later. This type of mill mainly spread from the Southwest of France, to Greece and Italy, and are frequently referred as the Mediterranean type of windmill.

2.2 Technical Development of windmills

In order to increase the performance of these type of structures, a systematic research and development were made, with an empirically founded evolution, based on experiment of new kinds of windmills and wind wheels. The first fundamental ideas concerning the design were raised in the Renaissance period, with Italian artists like Leonardo da Vinci and Veranzo, whose sketches and investigation, proposed various interesting design for vertical axis wind wheels. Only in the 17th and 18th century, wind technology was systematically considered for the first time. Names like Gottfried Wilhelm Leibniz (1646-1716), Daniel Bernoulli (1700-1782) and the mathematician Leonhard Euler (1707-1783), were the first to involve themselves in the matter, and to apply basic laws for the improvement of the sails for the windmills.
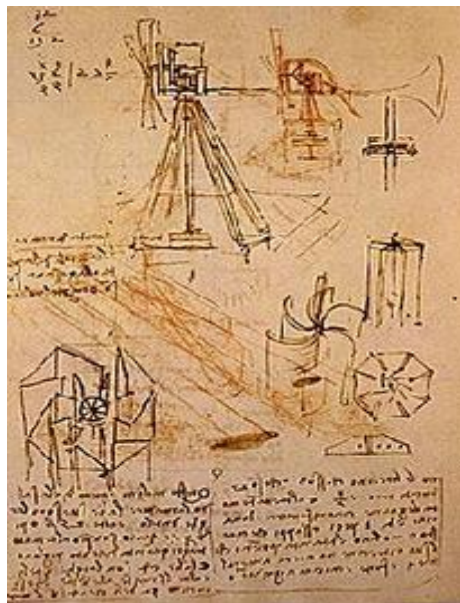
Figure 2-2 - Da Vinci's studies of a windmill (discoveringdavinci.com)

With the Dutch and British settlements in the New World, and the great movement to the west of the USA, a need for water that have to be pumped, opened a door for a new design of the windmills. They have to be light, easy to transport and assemble, should resist to the windstorms, and, most of all, be effective for many uses. In about 1850, Daniel Halladay found the first solution, which consists in a mechanism that can open a safety valve in the

case of over speeding. In low wind conditions, the blades pitch were kept at a shallow angle, and, with the increasing of the speed, the blades swung completely out of the plane of the wheel. This allowed a high torque even at low wind speeds, that were the exactly preconditions to drive a water pump.

Figure 2-3 - Wheeler Windmill with Eclipse design (artflakes.com)

With new technologies and materials, this rudimentary wind turbines evolved until nowadays for a very complex machine, able to generate an amount of electricity that can sustain hundreds of houses. But, in order to get the most advantage of the wind, in a higher altitude, these turbines have to be assembled in a high tower, capable of supporting all the stresses, principally the wind and the self-weight. They have been in a constant development, such as the blades, and now, new types of tower are needed, in order to get a better performance of the existent technology.

2.3 The tower

The high tower is an essential part of the horizontal-axis turbine, a fact that can be positive and at the same time a disadvantage. The costs are, obviously, a disadvantage, which can grow up to 30% of the overall turbine costs. As the height of the tower increases, transportation, erection and assembly become increasingly higher, but on the other hand, the energy yield also increases with the tower size.

The advantage of increased height was recognized and the old mill houses became more slender and with an aspect of a tower. In average, the increase of 1 meter in the tower height, brings a gain in the energy yield between 0.5% and 1%, depending on topographic conditions. So that, the optimum tower height can be determined from the point of economics, the increase in the cost of a higher tower must be compensated by an increase of the energy yield

of the turbine. But, the previous choice must be what type of tower is better for the programmed installation.

As a consequence of the development, designs and materials for towers increased in variety. Steel and concrete took the place of the wood, used to build the old windmills. In the early years, many designs and materials were tested in order to erect these towers, but the range of different types has narrowed to the most common, a free standing tubular steel tower, rarely made out of concrete.

2.3.1 Concrete Towers

Steel-reinforced concrete towers were very used in the 30' and were called "Aeromotors". Although the use of this type has a long tradition, nowadays they have been largely replaced by the tubular-steel towers prevailing today. Concrete allows to construct very high towers without the problem of the transportation, and the long construction time can be shortened by the use of prefabricated parts. These towers can be divided in two groups:

- Reinforced concrete towers – Towers were the steel reinforcement is just installed, and not prestressed.
- Prestressed concrete towers – In this case, the reinforcement is prestressed, sometimes with special tensioning elements, which make possible that the permissible stresses in the concrete can be increased.

The concrete towers that are made with one of the cases above have their advantages and disadvantages, and the decision for the best method to apply depends on the site, and the availability of an appropriate infrastructure. The cost comparison between the concrete tower types should not me made in a direct manner, but having in account the type of concrete construction or in comparison with tubular-steel or lattice towers. Despite of this, this towers have recently gained favour again for towers heights of more than 100 meters, with the particularity of using prefabricated concrete construction as preference.

2.3.2 Free-standing tubular-steel towers

Today, free-standing tubular-steel towers ate the preferred type of construction for commercial wind turbine installations. The advantage of this type of construction is the short on-site assembly and erection time, since the major part of the construction is made in the construction place, but as disadvantage, higher towers required a special road transportation due to the big size of these structures. However, the limit of the transport size is almost reached, which opens a new horizon for new design of wind towers.

The domain of the vibrational behaviour has made it easier to use this type of towers, so that very low design stiffness can be implemented. Higher towers of up to 100 meters are made of

individual sections that are bolted together and to the foundation in situ, so that no welding in the place of construction is required. Sometimes, when welding in the site of construction is possible, these towers are welded together from several segments in a horizontal position, being the tower hoisted in a single piece into a vertical position with the help of a small crane. The preference for this type of tower is also connected to the low prices of steel in the last twenty years.

Figure 2-4 – Free standing tubular-steel tower (wind-energy.tripod.com)

2.3.3 Lattice Towers

This is the simplest method of building high and stiff towers. By using a three-dimensional truss, it is possible to achieve very high towers, required for large turbines sited in inland regions. Lattice towers were the preferred design for the first experimental turbines and in the early years also were used for small commercial turbines. This type of tower is also used in another applications, as for energy transmission lines. Recently, the interest in these towers have increased, particularly in connection with large turbines with a hub height of 100 meters and more.

Lattice towers can be welded or bolted together from angled sections. Although this type of construction is not the cheapest one, the expenditure of material is less than in the case of tubular towers. The mass of the structure is less by up to 40%, but, as it have a more complicated assembly, it only traduces in about 10 to 20% compared to tubular steel towers. Only for increasing heights, the cost advantage becomes more relevant than this percentage.

The transportation for the site is easier, because it can be disassembled and moved to any desired site of construction. Very high lattice towers are feasible on remote sites, where heavy lifting equipment in not available. The longer assembly time and a great expenditure for maintenance are considered the biggest disadvantages of this type of structure, but it has no

great influence on the economic viability of the investment when compared to the other main costs.

One of the highest tower of a wind turbine to date with 160 meters was built with this type of structure, near Magdeburg in Germany. This tower consists of special hollow-section steel rods which are joined using high-strength extension bolts.

Figure 2-5 - Lattice tower of the Fuhrländer W2E (Hau, 2013)

2.3.4 Hybrid Lattice-Tubular towers

As stated above, the use of hybrid towers is possible to achieve greater heights for the turbine shaft. This type of towers is composed of 3 parts, the lower lattice part fixed to the foundation and assembled at the installation site, a piece of tubular tower consisting of several parts bolted together, as happens in most tubular towers, and a transition piece which ensures the connection and transmission of efforts between the two main parts.

A tower of this kind was recently installed at the wind farm in Gujarat, India. It is expected that this new type of towers produces about 10 to 12% more energy, because gains against the normal towers more than 40 meters in total height, with a combined height of 120 meters against the 80 meters of most tubular towers, therefore an ideal bet for low wind areas, due to its superior performance, with a potential to be installed in all parts of the world, without having to look for places where the wind speed is high. These towers can be climbed from the

inside, and have platforms inside the tubular part for maintenance and repair work, but also to maintain all the equipment necessary for its operation.

Figura 2-6 - Suzlon Hybrid Lattice-Tubular Tower (www.suzlon.de)

2.4 Increasing the Height with Different Tower Concepts

As we have seen before, in the initial phase of modern wind turbines and wind energy, the larger wind turbines were built with comparatively low towers. With more sophisticated technology and weaker inland wind regions, the height of the towers increased significantly, and now, towers with 100 meters or more were found to be a decisive factor for the more economical utilization of wind energy. On the other hand, with the raise of the high, the costs of the towers will naturally increase. However, the different types of tower show a different relation between the height and the cost, being some of them better for higher constructions than others.

The structural mass of self-supporting tubular steel constructions, and the cost of this type of towers disproportionally increases with increasing height. Added to this is the fact that the tower base section size have already reached the limit size for road transport of approximately 4.5 meters. To overcome this restriction, towers have started to be built from slim u-shaped shells, forming a polygonal section on the base of this structure. With this, the economical factor is maintained in towers up to 140 meters high, with the disadvantage of the increase in hand work on the construction site that comes with the assembly of the different plates that complete the section. Another aspect that we cannot forget is that these type of structures are heavier when compared to other type of steel structures, such as lattice types, which cause an initial investment higher that other designs.

The lattice type of tower is more suitable for achieving heights above 100 meters, because the increase of the structure mass with the height is not very accentuated. In general, this type of construction only have 60% of the mass of a tubular steel tower. However, economically that difference only represents about 20% due to the higher difficult of assembly, and more labour work.
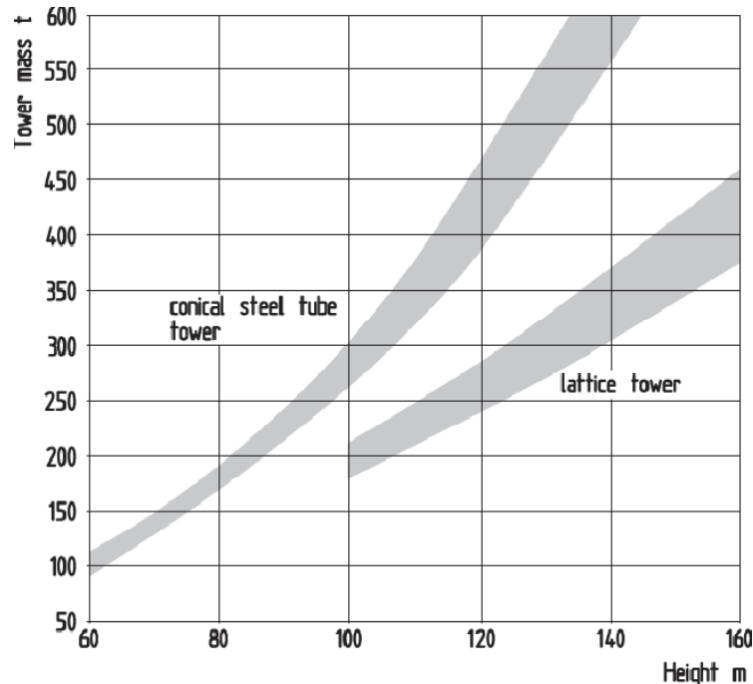
Figure 2-7 - Increase of the structural mass with height (Hau, 2013)

When we consider the concrete towers, then we face a different kind of problem. Although the tower mass is much higher, about 4 times when compared with steel towers, the increase with the height is less craggy. But the price of this type of tower is very affected by the distance between the construction site and the mixing plant. Although, the dynamic characteristics of the pure concrete tubes ate the limiting factor for the height increase. The first eigenfrequency tends to lower due to the higher mass on the upper section, becoming very difficult to avoid resonant problems.

The hybrid type seems to be the best way of construction, at least for towers height above 100 meters. There are a lot of hybrid towers installed, made from a prestressed concrete tower, assembled from pre-fabricated elements, which compound the base of the tower, with a tubular steel tower of about 25% of the total height. These types of tower are being used by ENERCON, for towers with more than 100 meters.
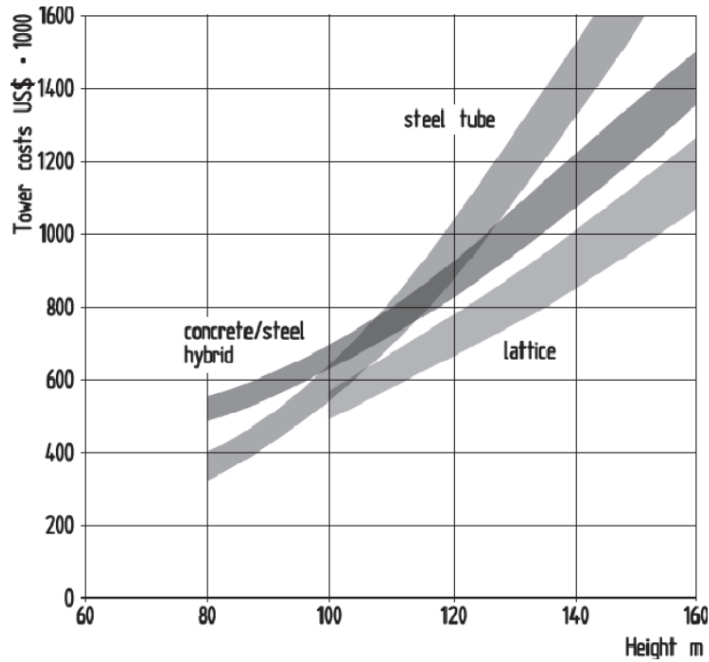
Figure 2-8 - Tower costs in dependence of high for a 3 MW wind turbine (Hau 2013)
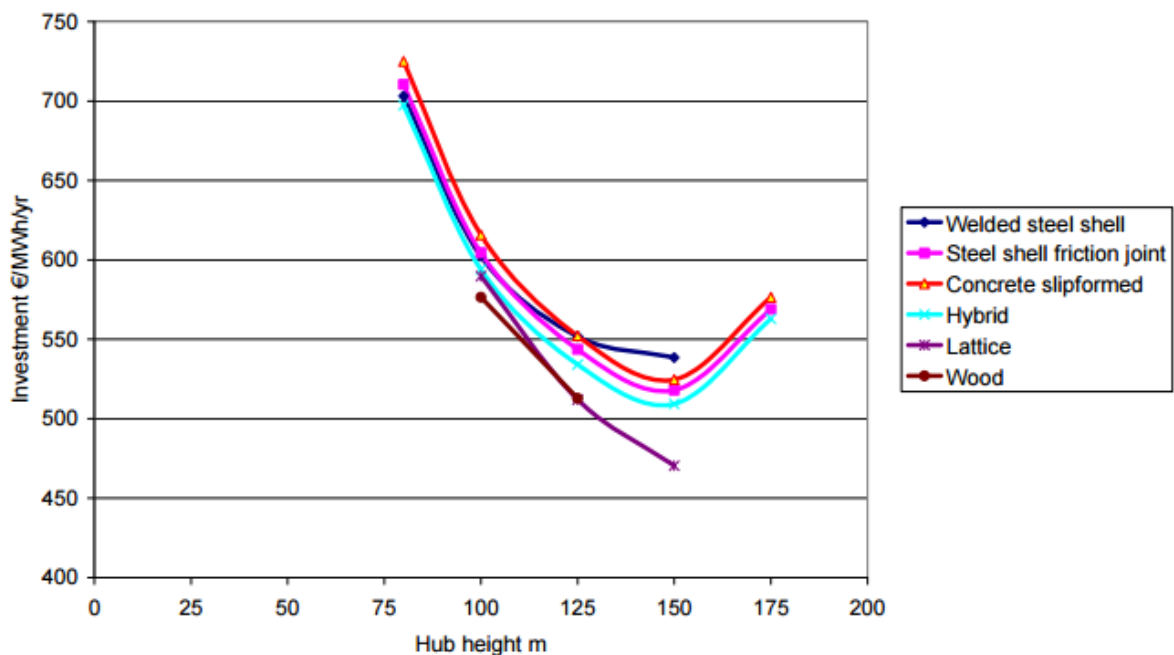
Figure 2-9 - Tower alternatives for 3 MW wind turbines (Vindforsk project)

Whit this analysis, is possible to conclude that the best solutions for the wind towers are the lattice construction and the tubular steel towers. A hybrid solution between these two types seems a promising option for higher towers, because we can put together the better of each one of them. A base from a lattice structure, whit higher hardness and a lower total mass, and an upper part made from a tubular part that can reach great heights. This is the study case in the master thesis, in order to perform an optimization for this new type of support for wind turbines.

João Rafael Branquinho Maximino   17

3 BACKGROUND THEORY

3.1 Load cases

Generally, for this kind of structures, extreme and normal wind conditions are defined by the highest speed condition occurring in a 50 years return period and a 1 year return period, respectively. When measuring this loads, they can be distributed by the ones that result from the interaction of the wind with the turbine, and the direct effect of the wind on the tower, that are combined appropriately to simulate the situation when they occur simultaneously.

3.1.1 Wind loads

The forces that act on the rotor and hub, that are transferred to the foundations by the tower, are a result of the effect from the wind, mass and elastic forces. The loads that result from this forces might be grouped into the next categories:

 ➢ Aerodynamic loads from a steady wind and centrifugal forces, generating a stationary load;

 ➢ A stationary, but spatially uneven flow field that causes cyclic load changes on the turning rotor;

 ➢ The mass forces from the rotation of the blade, causing periodic loads;

 ➢ The rotor is also exposed to random loads, that are caused by the wind turbulence;

Figure 3-1 - Representation of the loads on a wind turbine

The tower loading is bound to the type and the dynamic characteristics of the tower and the power of the turbine installed and supported. According to the situation, we can define two groups of load for the wind, one for operations conditions, and another for stationary position of the turbine, plus also consider another two groups for the fatigue effect and for the earthquake loads.

For extreme wind load in non-operating conditions, EW, the load combination includes loads on top of the tower and wind load distributed along the tower h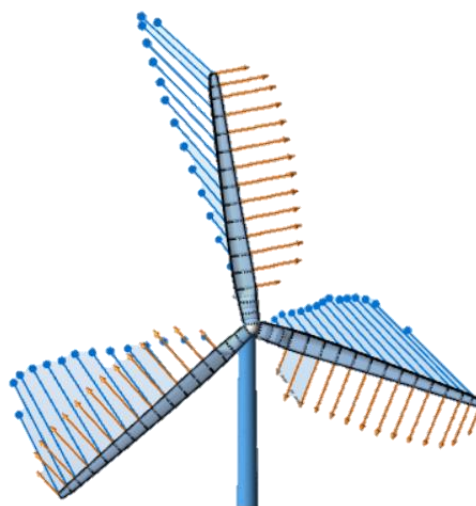eight. For this condition, the turbine is in parked position, subjected to steady wind speed of 42.5 m/s measured at hub height, averaged every 10 minutes, according to the definition of a turbine of class II. The type of structural analysis is the ultimate limit state, related to material and to structural stability, using the partial safety factors equals to 1.35 for the unfavourable actions and a value of 0.9 for favourable actions. In the case of extreme wind load in operating conditions, EO, the loads on the top of the tower may contain effects of faults in the operation of the turbine. The maximum wind speed considered on the hub for the load values is 33 m/s, corresponding to 20.8 m/s defined at 10 meters height, as recommended in EN1991-1-4.

Load Direction	EW	EO
Fx_{top} (KN)	578	1065
Fy_{top} (KN)	578	1065
Fz_{top} (KN)	-5000	-4879
Mx_{top} (KN.m)	28568	14987
My_{top} (KN.m)	28568	14987
Mz_{top} (KN.m)	5834	3966

Table 1 - Load Values for Wind Effect

3.1.2 Fatigue load and Earthquake load

The wind towers are likely to suffer fatigue damage and, by that, these structures must be checked for fatigue limit state. This load is related to the number of cycles (N) and the amplitude (S). These S-N curves are calculated for a year basis and then extrapolated for the life time of the turbine, approximately 20 years. To obtain the load values, an approximation was made, having in account the Damage Equivalent Load (DEL). This load introduces the same damage as S-N curves on the structure. Another dynamic load that cannot be waived is the earthquake loading, using the elastic displacement response spectrum, defined according the EN1998, with a peak ground acceleration of 0.2g. For the tables used, the behaviour factor was considered as q=1, a terrain of the type B, 2% damping for steel towers, 3% for hybrid towers, and is obtained by the super position of the seismic load effect with 30% of wind load on tower base.

3.2 Buckling analysis and strength of plates

According to EN 1993-1-6, buckling is an ultimate limit state where the structure suddenly loses its stability under membrane compression and/or shear. It leads either to large displacements or to the structure being unable to carry the applied loads. Is one of the most important part of analysis in thin walled members, which nowadays are used in several practical applications. The wide application of shell structures is sustained by the following favourable factors (Martins, J.P. 2013):

➢ Efficient load carrying performance;

➢ High strength vs. weight ratio; shell structures may be optimal structures;

➢ High values from an architectural point of view, once they can be easily integrated in urban and landscape areas;

However, shell structures are very slender structures and very sensitive to initial imperfections, which brings issues that must be considered when predicting the overall behaviour. By that, is important to have in account that the buckling resistance can be significantly lower than the theoretical buckling load, calculated from EN1993-1-3.
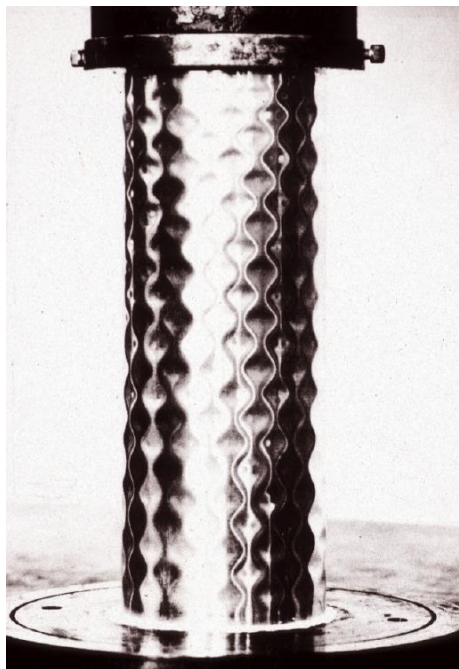

Figure 3-2 - Buckled thin unstiffened axially compressed cylindrically shell
(shellbuckling.com)

The En1993-1-6 shows a sequence of analysis to be performed. This sequence tries to systematize the various levels of analysis, in order to facilitate the communication between engineers, researchers and other people who are involved in the development of better

formulas for thin walled shell structures. The more specific the analysis, better is the approximation to the real values.

Linear analysis (LA) are applied to the perfect structure as a linear elastic eigenvalue calculation. This type of analysis have been subject to numerous research papers, principally due to their accessibility to analytical solutions. Geometrically nonlinear analysis (GNA) is applied on the pre-buckling state of the perfect structure, as an elastic material. This can be considered a refinement of the LA, anyhow, for elastic cylindrically shells, the results of these two methods bring similar results.

The third type is a geometrically and material nonlinear analysis (GMNA), that contains the effect of plasticity. Is an analysis based on shell bending theory applied to the perfect structure, using the assumptions of a nonlinear large deflection theory for the displacements and a nonlinear elasto plastic behaviour for the material. Geometrically nonlinear analysis with imperfections included (GNIA) is similar to a GNA analysis, but adopting a model for the structure that somehow includes the imperfect shape, with intentional deviations from the ideal shape of the structure. These imperfections may also cover the deviations in boundary conditions and the ones that result from the effect of residual stresses.

Last, but not the least, geometrically and materially nonlinear with imperfections analysis (GMNIA), gets together the characteristics of GMNA and GNIA, where the principles of shell bending theory are applied to the imperfect structure, including the theories presented before for the displacements and the material law. As explained before, shell structures are very sensitive to imperfections, so, by that, GMNIA is performed with the help of finite element software capable to introduce the imperfect model. In order to introduce the imperfections in the model, there are 3 possible ways:

- ➢ Realistic geometrical imperfections, when the real imperfections of the structure can be accurately measured;

- ➢ Worst geometrical imperfections when the worst pattern of imperfection in introduced in the structure

- ➢ Stimulating geometrical imperfections when a simple substitute for the imperfections can be implanted and stimulate the shell buckling behaviour. Tis process has to be calibrated, in order to get a closer approximation of the real imperfection and buckling behaviour.
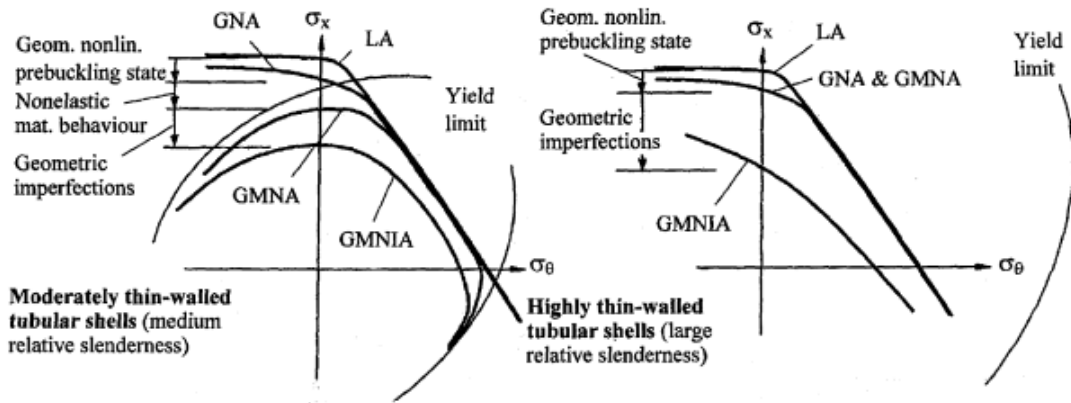
Figura 3-3 - Sequence of buckling analysis - The resistance is reduced with growing reality level (Th.A. Winterstetter, 2002)

The study of these type of structural solution has been developed in many years, and many design guides and rules are available. In 1891, Bryan proposed the elastic critical buckling stress for a plate (1), multiplying the classic Euler critical stress, calculated by the equation number (2) by the elastic buckling coefficient K_σ.

$$\sigma_{cr} = k_\sigma * \sigma_E \tag{1}$$

$$\sigma_E = \frac{\pi^2 * E}{12 * (1 - v^2)} * \left(\frac{t}{b}\right)^2 \tag{2}$$

Where t is the thickness of the plate, b is the width of the plate, E is modulus of Elasticity and v is Poisson's ratio.

In order to get a more accurate solution, the studies and researches were motivated by obtaining a more precise elastic buckling coefficient. In 1943, Stowell in his report, presented that the critical compressive stress for an infinitely long curved plate, is given by the following formula: (Stowell, 1943)

$$\sigma_{cr} = \frac{K_\sigma * \pi^2 * R * t^2}{12 - (1 - v^2) * b^2} + \frac{\theta^2 * E}{\pi^2 * K_\sigma} \tag{3}$$

And for larger curvature, the formula:

$$\sigma_{cr} = \frac{K_\sigma * \pi^2 * R * t^2}{12 - (1 - v^2) * b^2} * \frac{1 + \sqrt{1 + \frac{48 * (1 - v^2)}{\pi^4}\left(\frac{b^2}{K_\sigma * r * t}\right)^2}}{2} \tag{4}$$

However, the author indicates that the formula presented above for the larger curvature not always brings good and accurate results, when compared with experimental tests, a fact that was confirmed by other researchers. These errors were only solved when the imperfection sensitivity was introduced, and with knowledge that the critical stress was different from the ultimate stress, a fact that was proved by Dudiansky and Hutchinson in 1964.

More recently, in 2001, Domb and Leigh used a finite element technique to refine Batdford´s curves that have been presented in 1947, and obtain more accurate values for the buckling coefficient of cylindrically curved panels. The results are demonstrated in the following formula: (Martins, J.P. 2013)

$$k_\sigma = \begin{cases} 10 * \sum_{i=0}^{i} c_i [\log(Z_b)]^i \; if \; 1 \le Z_b \le 23,15 \\ c(Z_b)^d \; if \; 23,15 \le Z_b \le 200 \end{cases} \tag{5}$$

$$Z_b = Z * \sqrt{1 - v^2} = \frac{b^2}{r * t} \sqrt{1 - v^2} \tag{6}$$

In 2013, J.P.Martins et al, proposed an extension to the dimensioning rules of EN1993-1-5, related to eigenvalue analysis of cylindrically curved panels. In this report, a numerical study on the elastic buckling behaviour of simply supported cylindrically curved panels, including the influence of the curvature, aspect ratio and loading type, with a variation of loads since pure compression to full in-plane bending (Martins, 2013).

The panels were divided into two types, short curved panels (α<1) and long curved panels (α>1), being the factor α=a/b for a being the length of the plate and b the width of the plate under analysis. This division is necessary due to the fact that minimum elastic critical stresses occurs for panels with α<1 (the higher the curvature, the shorter the panel is for a minimum buckling coefficient).

With that, for short curved panels, buckling coefficient is defined by different combinations of the curvature parameter (Z), and the type of loading (ψ), as seen on Figure 3-4. Comparing the results obtained with numerical simulations, the maximum absolute error is 3.79%. For the long panels, a correlation factor is introduced, multiplied by the buckling coefficient, taking into account the increase in the elastic critical stresses due to the loading type and curvature. In this case, the maximum absolute error obtained during this calibration process is 3.35%. The results are presented on Figure 3-5.
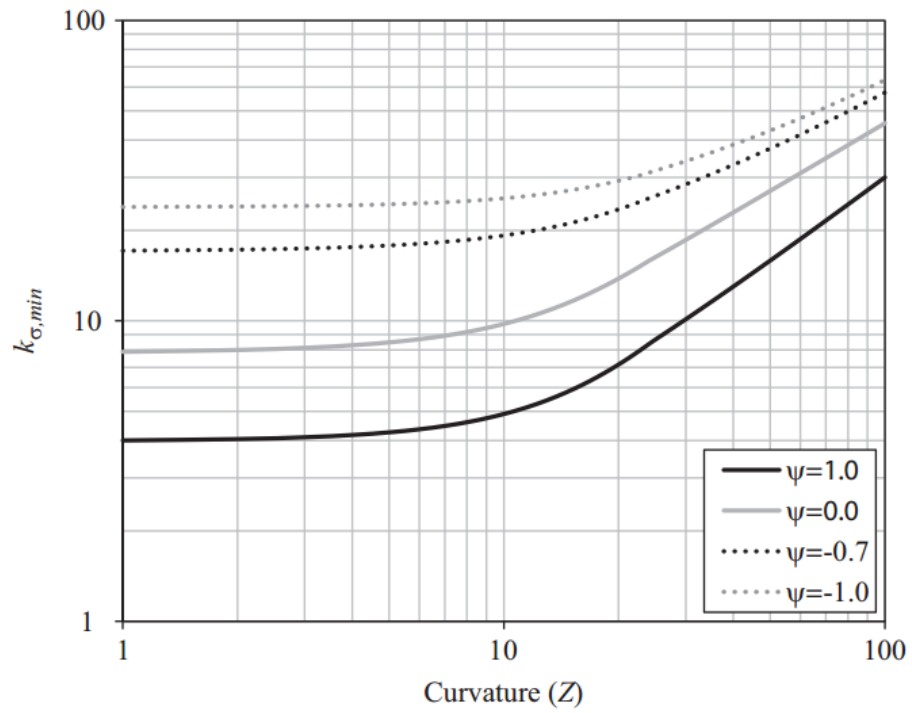
Figure 3-4 - Kσ for different values of ψ and curvature Z (Martins, 2013)
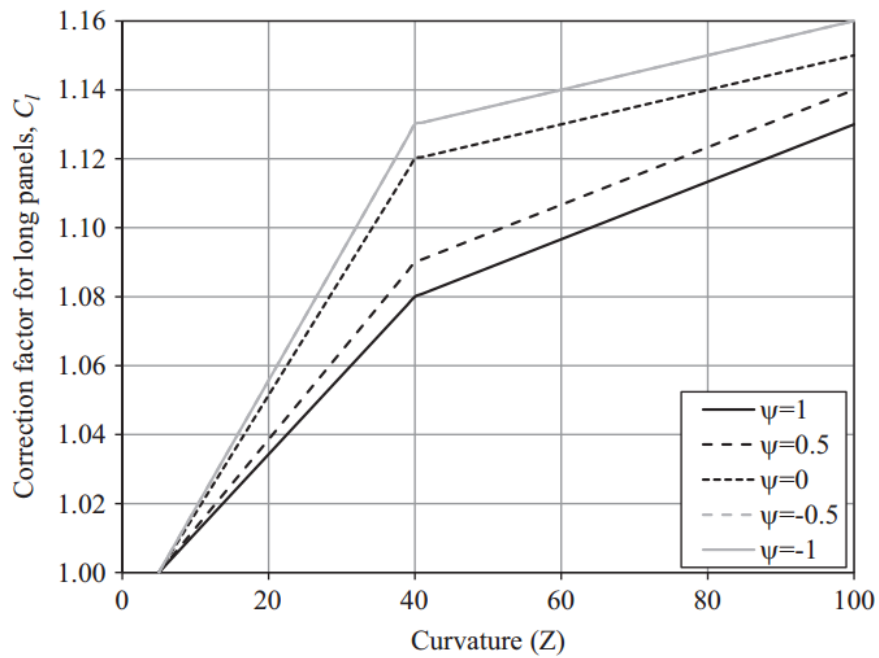
Figure 3-5 - Correlation factor, Cl, for long panels (Martins, 2013)

4 CONCEPTUAL MODEL AND DESIGN OF THE LATTICE TOWER

4.1 Design Requirements

After an introduction of the different types of wind towers and the knowledge that exists and let us go farther in using new structures, this thesis will now be focused on comparing two different structures, where the number of supports and levels will be changed, in order to get the best solution for this new kind of structures. In both of the structures, the supports are inserted in a circumference with 60 meters of diameter, equal to the total height of the lattice. The upper part has a diameter of 4.5 meters in order to fit the base of the tubular steel tower. The transition piece that unites the two types of structure will not be studied in this thesis.

The structure will be divided by horizontal plans, and, as higher the height of the tower, the smaller the distance between this plans, in order to increase the stiffness of the tower in the upper part. However, in order to make the assembly easier, the principal chords, which are the ones that support the other bars and are connected with the foundation, will only be divided in one horizontal plane that is situated at 46 meters in the six supports structure and 43 meters in the structure with 8 supports. With the optimization in mind, the structures will be dimensioned with 6 and 8 supports, and the level of the horizontal plans will also change. By that, 6 different structures will be dimensioned in an early stage using circular hollow sections, to decide the better combination between the two variables. After that, the best tower for each number of supports will be also optimized using a new type of cross section, whose properties will be presented further on.
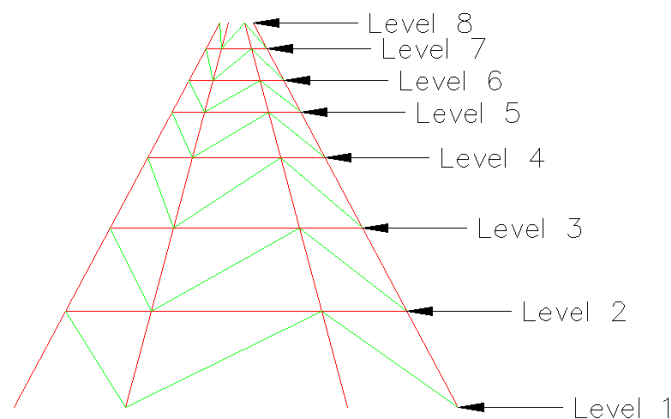
Figure 4-1 - Drawing of the Lattice Structure to label the levels

	G_6_1	G_6_2	G_6_3	G_8_1	G_8_2	G_8_3
Level 1 (m)	0	0	0	0	0	0
Level 2 (m)	12	15	18	12	15	18
Level 3 (m)	24	28	32	24	28	32
Level 4 (m)	36	39	42	36	39	42
Level 5 (m)	44	46	50	44	46	50
Level 6 (m)	50	51	56	50	51	56
Level 7 (m)	55	56	60	56	56	60
Level 8 (m)	60	60	-	60	60	-

Table 2 - Horizontal plans dividing the structures

The properties of the material, S355NH/NHL, used for the dimensioning process, guarantee the requirements established by EN1993:1:1. The nominal values for the yield strength, "*fy*" and ultimate strength "*fu*", is defined according the EN10210-1, as the Eurocode recommends. These values are displayed on Table 3.

fy(N/mm^2)	355
fu(N/mm^2)	490
E (N/mm^2)	210000
G (N/mm^2)	81000
ν	0.3
α (C^{-1})	$12*10^{-6}$
ρ (Kg/m^3)	7850

Table 3 - Steel Properties

4.2 The Conceptual Model

Structural analysis was performed using the software "Autodesk Robot Structural Analysis Professional 2014". On the models used for the optimization, the transition piece, that has the function to link the lattice structure to the tubular part and to secure the transmission of efforts, was performed by the introduction of a rigid link on the top of the lattice, where the tubular part inserts. The introduction of only this type of connection between the two structures brings the result that is closer to the reality, when a real connection piece is inserted.

In order to make the tower to behave like a truss structure, all the horizontal bars and the diagonal braces where released, so, by that, they are only subjected to axial effort, which also

makes the dimensioning process easier. This assumption was possible because in the final structure, all the connections will be bolted, without welding, which gives this characteristic to the bars not only in the model, but also when they are being used in the real structure. For the supports, the major part are released, but some of them are maintained fixed, in order to avoid displacements in some critical directions. The fact of these few are restrained doesn't affect the dimensioning that much, because the bending moment on the basis of the structure doesn't represent a substantial value.

4.3 Structural analysis

The global analysis of a steel structure depends fundamentally of the stiffness and deformability, but also from the global stability and the stability of the different parts, the behaviour of the cross section, the type of connection between the bars, the imperfections that can result from various factors, and many other factors. By that, in the definition of the correct analysis mode, all these aspects have to be taken into account. According to the EN1993-1-1, defines what type of analysis should be performed, comparing the elastic critical buckling load of the structure with the design loads applied. On the same part of the EN1993-1-1 (5.2.1), is also referred if a second order analysis should be performed. This happens when the relation between the loads presented before is smaller than 10.

$$\alpha_{cr} = \frac{F_{cr}}{F_{Ed}} \geq 10 \; for \; elastic \; analysis \tag{7}$$

In the structures analysed in this thesis, this relation is not achieved, so a non-linear analysis has to be performed in order to get the proper efforts on the structure. After that, the cross sections and the element can be verified, with special attention on the buckling response of the longer members.

To validate the results, a numerical analysis will be performed for one bar, which makes part of the chords, subjected to axial effort but also bending moment. The same process was performed to all the bars in the six different structures, in order to get all cross sections dimensioned according the EN1993-1-1. The section verified in the following design procedure will consist of the top part of the chords on the G_8_3 geometry. The values of the efforts will be presented on Table 4 and the characteristics of the cross section are displayed on Table 5.

Effort	Value
N_{Ed} **(KN)**	12543.95
M_{yEd} **(KNm)**	522.14
M_{zEd} **(KNm)**	-60.34
V_{yEd} **(KN)**	13.49
V_{zEd} **(KN)**	116.73

Table 4 - Efforts applied on the member

Outside Diameter	Thickness	Mass	Area	Inertia	Radius of Gyration	Elastic Modulus	Plastic Modulus
D (mm)	T (mm)	M (Kg/m)	A(cm^2)	I (cm^4)	I (cm)	Wel (cm^3)	Wpl (cm^3)
610	25	361,13	459,45	196906,44	20,7	6455,9	8560,83

Table 5 - Cross section properties

4.3.1 Cross Section Class

According to the table 5.2 of the EN1993-1-1, for a tubular section, the relation between the different classes is given by the following:
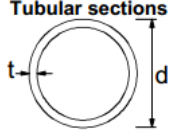
Figure 4-2 - Maximum ratios between the diameter and thickness (EN1993-1-1)

$$\frac{d}{t} = \frac{610}{25} = 24,4 \leq 50 * 0,66 = 33 \qquad (8)$$

As the ratio between the diameter and the thickness is smaller when compared to the limit of the class 1, the cross section resistance is based on a plastic design, and the plastic properties can be used.

4.3.2 Compression verification

As the cross section used is from class 1, the compression can be verified using the equation (6.9) and (6.10) of the EN1993-1-1.

$$\frac{N_{Ed}}{N_{c,Rd}} \leq 1 \ and \ N_{c,Rd} = \frac{A * f_y}{\gamma_{M0}} = 16310,8 \ KN \tag{9}$$

$$\frac{N_{Ed}}{N_{c,Rd}} = \frac{12543,95}{16310,8} = 0,769 \leq 1 \tag{10}$$

4.3.3 Shear force verification

According to the division 6.2.6 of the EN1993-1-1, the design value of the shear force at each section should satisfy the following expression.

$$\frac{V_{Ed}}{V_{pl,Rd}} \leq 1 \tag{11}$$

By that, in the same division of the referred norm, the plastic shear resistance is given by the following.

$$V_{pl,Rd} = \frac{A_v * (f_y / \sqrt{3})}{\gamma_{M0}} \ and \ A_v = \frac{2 * A}{\pi} \tag{12}$$

By that, the shear resistance can be compared with the applied and the result is shown next.

$$\frac{V_{Ed}}{V_{pl,Rd}} = \frac{116,73}{5995,1} = 0,02 \leq 1 \tag{13}$$

When in a cross section bending and shear force are present, an allowance should be made on the bending moment resistance. Although in this situation that occurs, as the shear force is less than half of the plastic shear resistance, its effect on the bending moment resistance may be neglected. The same situation happens for torsion and shear effort, but once there are no torsional efforts in this chord, the plastic shear resistance doesn't need to be affected.

4.3.4 Bending and axial force

Once the member is subjected to axial effort and bending moment, instead of verifying just the bending moment, the value of the ratio of the compression effect will also affect the

bending moment resistance of the cross section. For circular hollow sections with constant thickness, the value of the resistant bending moment is calculated by the following expression. After calculating the proper resistant bending moment, it´s possible to verify if the section has the ability to support the bending moment applied.

$$M_{N,y,Rd} = M_{N,z,Rd} = \frac{W_{pl} * f_y}{\gamma_{M0}} (1 - n^{1,7}) = 1094,29 \ KNm \tag{14}$$

$$\left(\frac{M_{y,Ed}}{M_{N,y,Rd}}\right)^2 + \left(\frac{M_{z,Ed}}{M_{N,z,Rd}}\right)^2 = \left(\frac{522,14}{1094,29}\right)^2 + \left(\frac{60,34}{1094,29}\right)^2 = 0,231 \leq 1 \tag{15}$$

4.3.5 Buckling analysis – Uniform members in bending and axial compression

In the following verification, the stability of the member will be taken into account due to the effect of the buckling factor introduced, that will reduce the capacity of the section in supporting efforts, affecting the resistant axial effort. This factor is dependent of the inertia of the section and also the length of the member in analysis. The member that is into analysis in this demonstration have a length of 4.7 meters. For longer members of the structure, situated on the bottom part of it, this factor is very important, because it will reduce significantly the resistance of the cross section. To calculate this value, it will be use the part 6.3.1.2 of the EN1993-1-1. In order to define the factor, the appropriate buckling curve is needed, in order to get the correct value of the resistance. Once we are facing a hot finished hollow section, the correct buckling curve is the "a", with the correspondent value of 0.21. The value of the factor will also be equal in both directions, because it's a circular hollow sections with constant thickness. In the following part not only this factor, but all the parameters needed to complete this verification will be presented in a resumed way.

$$\chi = \frac{1}{\Phi + \sqrt{\Phi^2 - \bar{\lambda}^2}} \quad \text{but } \chi \leq 1,0 \tag{16}$$

In order to determine the slenderness, the critical load is needed. To calculate his value, the Euler formula will be used, and present in the next formula.

$$N_{cr} = \frac{\pi^2 * E_t * I}{L_e^2} = 204250,87 \ KN \tag{17}$$

$$\bar{\lambda} = \sqrt{\frac{A * fy}{N_{cr}}} = 0,283 \tag{18}$$

$$\Phi = 0,5 * \left[1 + \alpha * \left(\bar{\lambda} - 0,2\right) + \bar{\lambda}^2\right] = 0,549 \tag{19}$$

With all the parameters calculated, it's easy now to achieve the value of the buckling factor.

$$\chi = \frac{1}{0,549 + \sqrt{0,549^2 + 0,283^2}} = 0,981 \tag{20}$$

In this member, as said before, this factor doesn't have such a big influence on the resistance of the member, because it has a high moment of inertia and it's a short member, with only 4.7 meters long, although it doesn't mean that this members can be exempted from this procedure.

With the buckling factor that will affect the compression resistance, it's now necessary to calculate the factors that will affect the bending moment resistance. This factors can be obtained using the Annex B of the EN1993-1-1 that refers to the method 2 present in this code, and the factors k_{ij} will be obtained. In the next steps the tables displayed in the Eurocode will be presented, and the final values for this factors calculated.
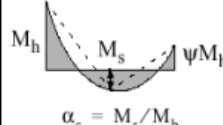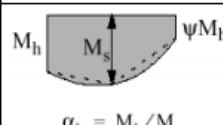
Moment diagram	range		C_{my} and C_{mz} and C_{mLT}	
			uniform loading	concentrated load
M, ψM	$-1 \leq \psi \leq 1$		$0,6 + 0,4\psi \geq 0,4$	
M_h, M_s, ψM_h $\alpha_s = M_s/M_h$	$0 \leq \alpha_s \leq 1$	$-1 \leq \psi \leq 1$	$0,2 + 0,8\alpha_s \geq 0,4$	$0,2 + 0,8\alpha_s \geq 0,4$
	$-1 \leq \alpha_s < 0$	$0 \leq \psi \leq 1$	$0,1 - 0,8\alpha_s \geq 0,4$	$-0,8\alpha_s \geq 0,4$
		$-1 \leq \psi < 0$	$0,1(1-\psi) - 0,8\alpha_s \geq 0,4$	$0,2(-\psi) - 0,8\alpha_s \geq 0,4$
M_h, M_s, ψM_h $\alpha_h = M_h/M_s$	$0 \leq \alpha_h \leq 1$	$-1 \leq \psi \leq 1$	$0,95 + 0,05\alpha_h$	$0,90 + 0,10\alpha_h$
	$-1 \leq \alpha_h < 0$	$0 \leq \psi \leq 1$	$0,95 + 0,05\alpha_h$	$0,90 + 0,10\alpha_h$
		$-1 \leq \psi < 0$	$0,95 + 0,05\alpha_h(1+2\psi)$	$0,90 - 0,10\alpha_h(1+2\psi)$
For members with sway buckling mode the equivalent uniform moment factor should be taken $C_{my} = 0,9$ or $C_{Mz} = 0,9$ respectively.				

Figure 4-3 - Table B.3 of the EN1993-1-1

The first parameter has to do with the bending moment diagram present in the member in analysis. In this case, the diagram is linear, and varies from 0 until 522.14 KNm in the y direction and from 0 to -60.34 KNm in the z direction, as shown on Figure 4-4.
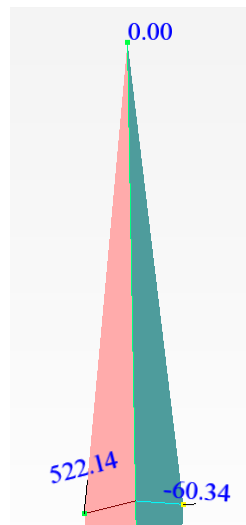
Figure 4-4 - Bending moment in y direction (red) and z direction (green)

Due to the fact that both diagrams start from 0, the parameter ψ is also equal to 0, because it refers to the relation between the smaller values of the bending moment with the higher value, in the element in study. As so, the parameters C_{my} and C_{mz} are equal to 0.6. With this two values, in now possible to achieve the factors k_{ij}, that will directly affect the bending moment resistance. The way to calculate this factors is presented in the table B.1. of the same Eurocode. As the section belongs to the class 1, it will be used the right column of the table presented on the Figure 4-5, for the RHS-sections.

Interaction factors	Type of sections	Design assumptions	
		elastic cross-sectional properties class 3, class 4	plastic cross-sectional properties class 1, class 2
k_{yy}	I-sections RHS-sections	$C_{my}\left(1+0,6\bar{\lambda}_y \dfrac{N_{Ed}}{\chi_y N_{Rk}/\gamma_{M1}}\right)$ $\leq C_{my}\left(1+0,6\dfrac{N_{Ed}}{\chi_y N_{Rk}/\gamma_{M1}}\right)$	$C_{my}\left(1+\left(\bar{\lambda}_y-0,2\right)\dfrac{N_{Ed}}{\chi_y N_{Rk}/\gamma_{M1}}\right)$ $\leq C_{my}\left(1+0,8\dfrac{N_{Ed}}{\chi_y N_{Rk}/\gamma_{M1}}\right)$
k_{yz}	I-sections RHS-sections	k_{zz}	$0,6\,k_{zz}$
k_{zy}	I-sections RHS-sections	$0,8\,k_{yy}$	$0,6\,k_{yy}$
k_{zz}	I-sections	$C_{mz}\left(1+0,6\bar{\lambda}_z \dfrac{N_{Ed}}{\chi_z N_{Rk}/\gamma_{M1}}\right)$ $\leq C_{mz}\left(1+0,6\dfrac{N_{Ed}}{\chi_z N_{Rk}/\gamma_{M1}}\right)$	$C_{mz}\left(1+\left(2\bar{\lambda}_z-0,6\right)\dfrac{N_{Ed}}{\chi_z N_{Rk}/\gamma_{M1}}\right)$ $\leq C_{mz}\left(1+1,4\dfrac{N_{Ed}}{\chi_z N_{Rk}/\gamma_{M1}}\right)$
	RHS-sections		$C_{mz}\left(1+\left(\bar{\lambda}_z-0,2\right)\dfrac{N_{Ed}}{\chi_z N_{Rk}/\gamma_{M1}}\right)$ $\leq C_{mz}\left(1+0,8\dfrac{N_{Ed}}{\chi_z N_{Rk}/\gamma_{M1}}\right)$
For I- and H-sections and rectangular hollow sections under axial compression and uniaxial bending $M_{y,Ed}$ the coefficient k_{zy} may be $k_{zy}=0$.			

Figure 4-5 - Table B.1 of the EN1993-1-1

Using the results shown previous on this demonstration, is possible to calculate the values of these parameters for this forces, as shown in the following

$$k_{yy}= \quad 0,639 \qquad\qquad k_{zz}= \quad 0,584$$

$$k_{zy}= \quad 0,383 \qquad\qquad k_{yz}= \quad 0,350$$

Another factor that is necessary in the lateral buckling χ_{LT}. However, once we are working with circular hollow sections, this factor takes a value equal to the unity, therefore is equal to 1. With all the parameters necessary calculated, is now possible to apply the equations 6.61 and 6.62 of the EN1993-1-1, and proceed to the member verification when subjected to compression and bending moment, having into account the buckling resistance.

$$\frac{12543,95}{0,981 * 16310,8} + 0,639 * \frac{522,14}{\frac{1 * 3039,1}{1}} + 0,35 * \frac{60,34}{\frac{1 * 3039,1}{1}} = 0,9 \qquad (21)$$

$$\frac{12543,95}{0,981 * 16310,8} + 0,584 * \frac{522,14}{\frac{1 * 3039,1}{1}} + 0,383 * \frac{60,34}{\frac{1 * 3039,1}{1}} = 0,89 \qquad (22)$$

As shown by the results, the relation between the efforts is smaller than one, which makes the element valid and capable to support all the efforts. With the same process made for all the elements in the structure, all the members presented are capable to secure the efforts applied.

Being the towers properly dimensioned, it's crucial to compare the solutions obtained by this models. In this first analysis, the comparison will be made by the total weight of the structure. Another important comparison in between the utilization ratio of the elements, in which, a higher average of ratio induces that the cross sections selected for the elements are appropriated and the dimensioning process was made correctly. However, this analysis will only be made further in this thesis, with the cross sections that are in study in this thesis. On **Table 6**, is shown the results for the total weight of the six structures used.

	G_6_1	G_6_2	G_6_3	G_8_1	G_8_2	G_8_3
Weight (Kg)	270846	278422	242884	267009	251113	262829

Table 6 - Total weight of the structures

As seen from the table above, the lighter are the G_6_3 and G_8_2. By that, these are the structures that will be given attention in the dimensioning with new cross sections and further for the connections design.

With that it's possible to conclude that the structure with only six supports is the lighter, although the profiles needed for this structure are bigger than the ones used in the 8 supported structure. One of the biggest problems for these structure was the effect of the buckling in the lower part of the structure, in special in the diagonals, represented as green on Figure 4-1, that leads to a bigger cross section area with also bigger inertia, in order to confront this problem. One solution is to adopt an X system for the bars in this part of the structure that will lead to a smaller length of the bars, and that way, the buckling effect can be reduced effectively.

5 CROSS SECTION - PROPERTIES AND DESIGN

5.1 Assembly of the cross section

As stated before in this thesis, the geometries presented so far were dimensioned with circular hollow sections, just to achieve a better geometry for the tower, instead of just choosing one geometry, which could lead us to a bad solution, in this case a much higher total weight. With that in mind, in the following chapter, the new cross sections properties and dimensions will be presented, in order to perform an analysis of the structures using the real sections.

The new tubular section used in this study consists of several separate parts, bolted together, to obtain a versatile section, easy to assembly and without the need of special conditions for the transport, as the ones that already limit the size of tubular steel wind towers. The choice of such section also takes into account a greater economy in carrying out the connections between bars, ease of assembly in situ, since it's only necessary to screw the two parts that make up the section. Another good property is, due to the fact that these cross section does not have welds in joints or any part, the fatigue effect on the structure is much smaller, one effect that is very important to have into account in structures that are submitted to cyclic loads, such as wind towers.
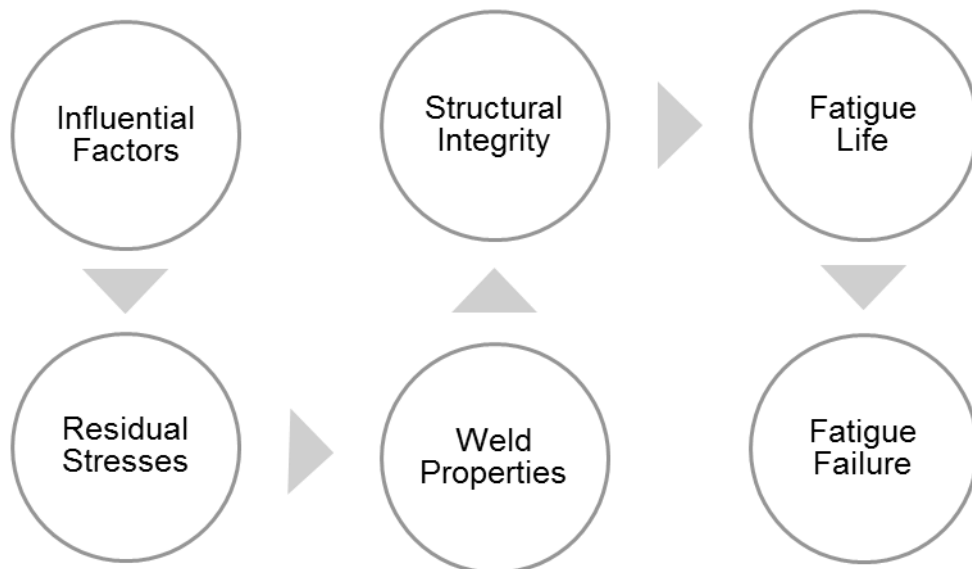

Figure 5-1 – Effect of residual stresses on a structure

In order to form the parts that compose the section, plates are bended, and therefore, not very large thicknesses for the elements were chosen, in order to facilitate the moulding process. To

obtain a flat area to locate the screws, the flat sheet bending process is better when compared to the process of welding a continuous element on half of a circular profile. In this way, it is possible to prevent the introduction of residual stresses on the steel that are a result of the welding process. These type of stresses are difficult to measure, and if they aren't properly accounted in the dimensioning of cross sections, they could compromise the performance and overall strength of the structure.
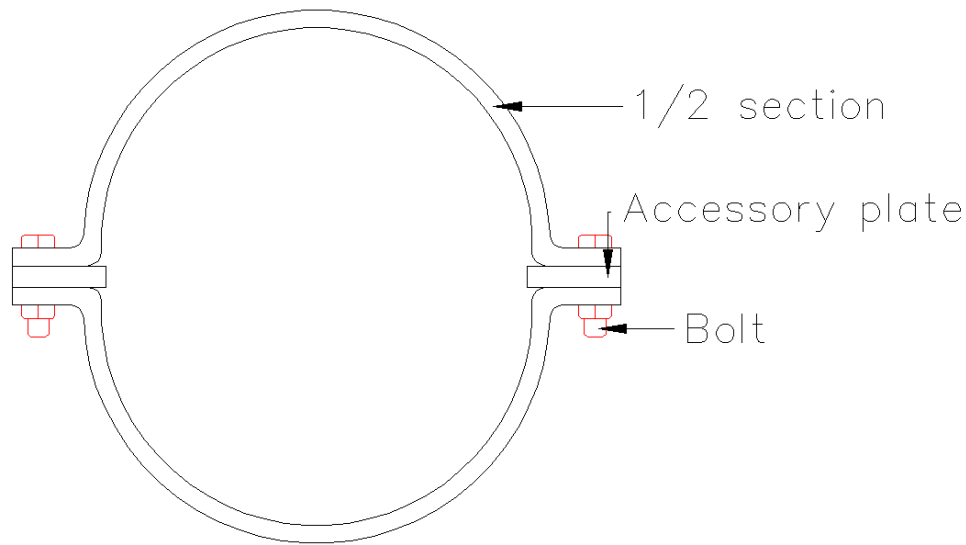

Figure 5-2 - Cross section parts and assembly

To make the connection between the bars of the structure, plates will be used common to the profiles, using bolts to link the bars to this plates. In order for the section to keep the characteristics along the entire length of the bar, the various parts that constitute the section are bolted together, maintaining a spacing of approximately 900 mm between the bolts, with the use of accessory plates in this areas, in order to get a constant space between the half parts, being this space equal to the thickness of the plate used to connect the different bars of the structure, plates that have a thickness of 20 mm. This type of connection along the length of the bars also allows to deal with this cross section as if they were a circular hollow section and not as simple plate, which brings a gain in the resistance of the cross section.

5.2 Cross Section Properties

After a brief presentation of how the cross section behaves and how to assembly the bars and the connections, it's now time to present the properties needed to make a correct design of the structure, as the area, moment of inertia, and also all the dimensions needed for the industry, concerning to build all the parts. To accomplish that, the sections will be divided in two parts. In first place, the dimensions of the diagonal and horizontal bars will be presented, and after that, the dimensions concerning the main chords. In this second part, special concerning has to

be made, due to the different angle between the connection plates, due to the different angle in the six and eight supported structure. To be possible to distinguish the sections used on both of the structures, the names presented on Table 7 will begin with an "S" for the six supported structure and with an "O" for the eight supported. In the Figure 5-3 are represented the different dimensions in a generic cross section. The properties of the different cross sections were obtained with resort to *Autodesk AutoCad* and *Autodesk Robot Structural Analysis*.
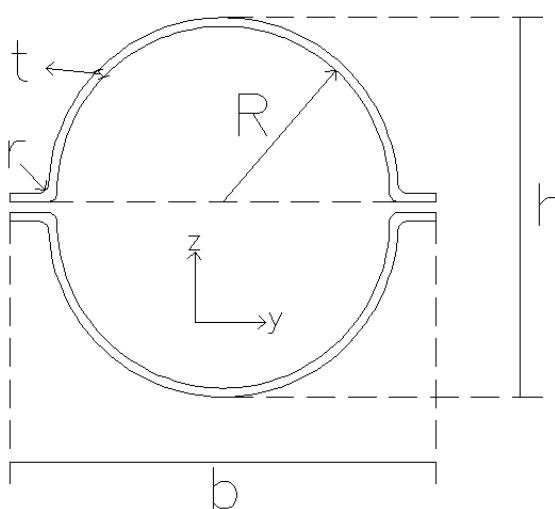
Figure 5-3 - Dimensions of the cross section – Horizontal and Diagonal

Section Name	h(mm)	b(mm)	R(mm)	r(mm)	t(mm)	A(cm^2)	Ix(cm^4)	Iy(cm^4)
Sa	396	480	172	8	8	106.15	21956.67	16720.29
Sb	440	520	192	10	10	144.68	35683.29	29649.55
Sc	456	540	202	8	8	120.01	32423.72	25849.76
Sd	544	680	238	12	12	219.97	81715.67	67849.85
Se	504	640	218	12	12	199.79	63820.00	52516.61
Sf	594	670	263	12	12	236.72	103471.55	89566.24
Sg	692	820	304	16	16	370.42	219611.51	187671.07
Sh	504	584	220	12	12	202.83	64869.16	53749.04
Od	365	445	152.5	10	10	122.38	20256.27	16526.38
Oe	500	580	220	10	10	168.32	53760.74	43941.58
Of	415	495	177.5	10	10	141.93	31701.61	24669.07
Og	340	420	140	10	10	114.59	16526.64	13325.39
Oh	602	730	259	16	16	348.45	170221.58	116973.47

Table 7 - Cross Section Properties – Horizontal and Diagonal

One important consideration about this section, it's the difficult to maintain a small thickness and at the same time to achieve high areas, without getting a class 4 section which lowers the resistance of the cross section. Another consequence of using this cross section in the big size of the parts were the bolts will be attached, in order to get the minimum required by the EN1993-1-8. By that, the area of this stiffeners will increase the area in about 15%, when compared to a similar circular hollow section, without having major effect in the inertia of the section on the principal direction, the y-axis. This will lead to a heavier structure, when compared to the circular hollow section.

Focusing on the chords, the cross section is divided in three separated parts, where two of the divisions are made to serve as support for two different bars and the other to increase the inertia in the principal direction and to further an easily bending process of the plates. The stiffeners in this bars will be bigger than the ones used in the ones presented before, in order to accommodate bigger bolts that allow the use of a lower number of these elements.
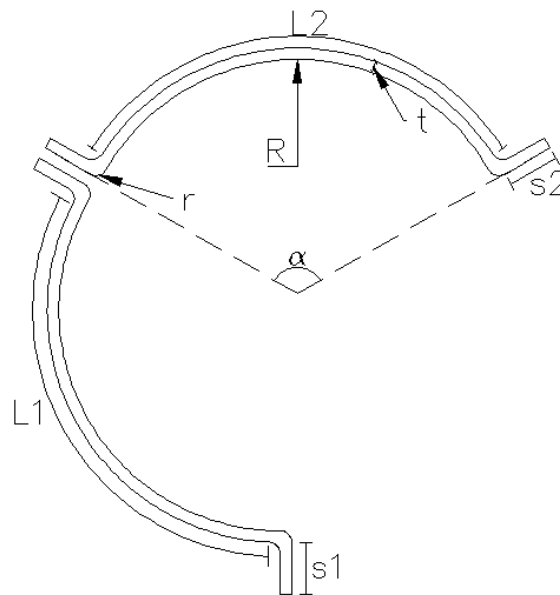
Figure 5-4 - Dimensions of the cross section – Chords

Section Name	S1	L1	S2	L2	r	t	R	α
Si9	70	799.7	70	799.7	20	20	380	120
Si92	70	799.7	70	799.7	20	20	380	120
Sj10	76.7	499.1	76.7	499.1	12.5	12.5	234	120
Oa2	83.4	465.7	95.6	570.7	12	12	243	135
Ob1	84	650.6	99.7	794.1	16	16	334	135
Oc1	84	650.6	99.7	794.1	16	16	334	135

Table 8 – Cross Section Properties - Chords

Section Name	A(cm²)	Iy(cm⁴)	Iz(cm⁴)	W_{ply}(cm³)	W_{plz}(cm³)
Si9	620.47	563358.64	562831.51	11132.41	12394.51
Si92	686.94	631506.24	631137.27	12455.06	13900.85
Sj10	268.03	102502.64	102126.51	2926.82	3163.79
Oa2	266.11	109077.29	102878.34	3167.13	2838.52
Ob1	449.69	323016.50	311042.16	7419.93	6747.65
Oc1	518.47	387087.86	360723.40	8890.85	7883.56

Table 9 - Cross Section Properties - Chords

With all the properties of the cross sections presented, it´s possible now to show where the different bars will be displayed on the structure. This will be presented along with some images, from the software used to design the structure.
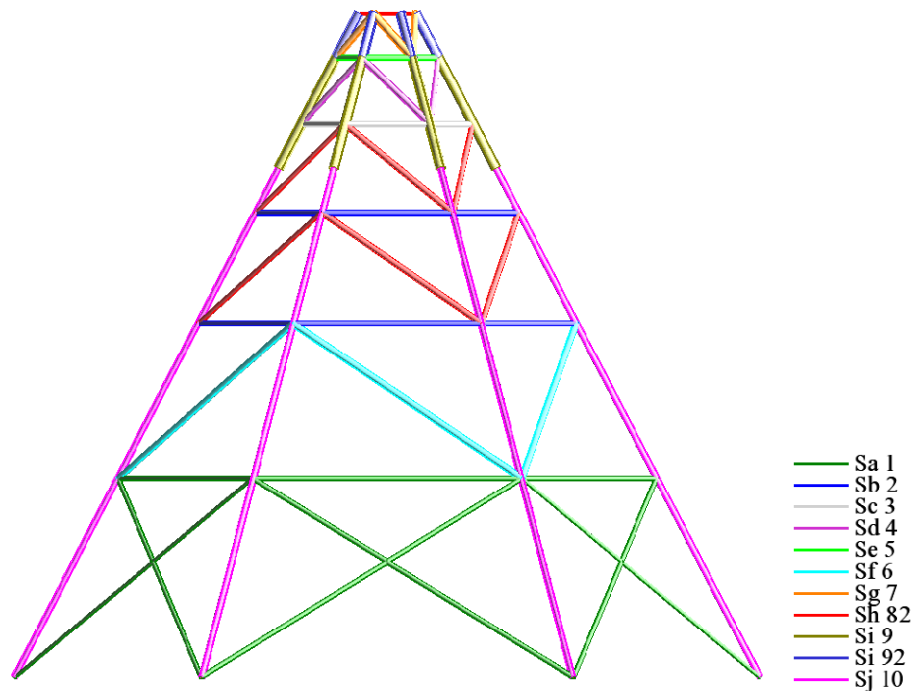

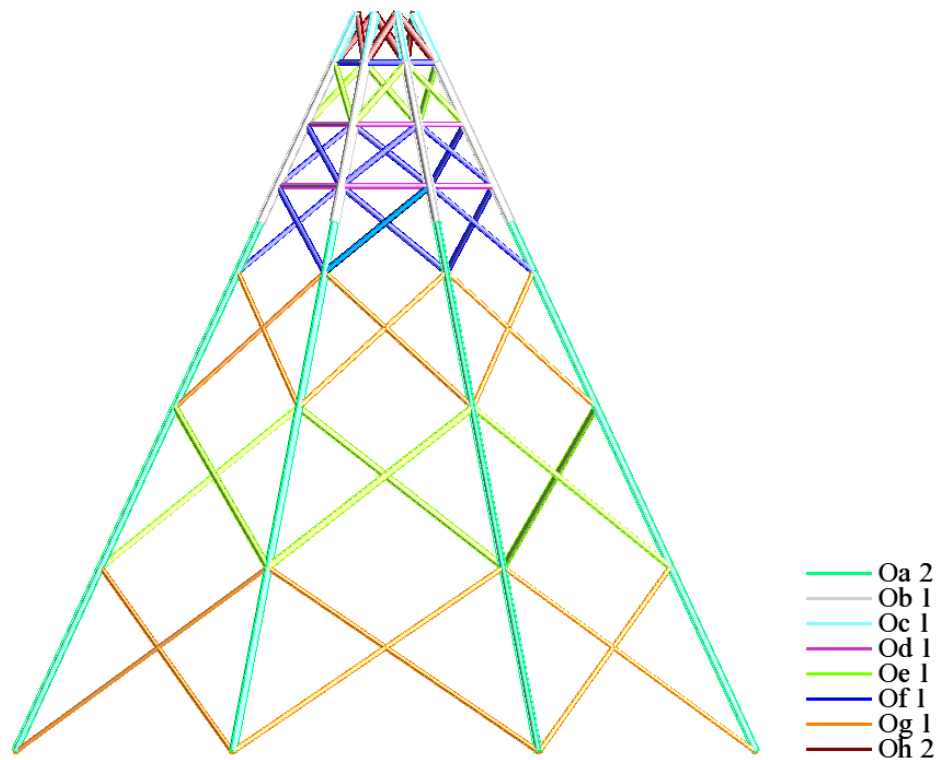Figure 5-5 - Legend of the different bars on six support structure

Figure 5-6 - Legend of the different bars on eight support structure

5.3 Design of the tower with new cross sections

As stated before, some of the members of the structure were very affected for buckling effects, due to the long length. In order to face that problem, some alterations were made to the structure. The most evident one is the addiction of another diagonal on the first level of the structure, so, in this way, the total length of the element is reduced by almost a half, which makes the elements less propitious to the buckling effect. In the eight supported tower, the horizontal bars in the bottom part were removed, since it's effect were not very present, and the efforts that were transmitted to this bars were absorbed by others elements, without the necessity to increase the area. However, in the upper part they remained, in order to give a higher stiffness to that part of the structure. With all the alterations made, it's now possible to make the dimensioning of the members with the respective cross section.

Once that in the previous part was presented the dimensioning of a chord, with axial effort and bending moment, now will be presented the dimensioning of an element only subjected to axial compression. The element belongs to the eight supported structure, more specifically the diagonal between level 7 and 8 of the geometry chosen, G_8_2, and the cross section is identified on Table 7 as "Oh". The shear force will be neglected since the effect on the structure is not determinative. Since one detailed dimensioning process was performed before,

the principal results of the dimensioning with this new cross section will be presented in the following steps. On is presented the properties needed for this design.

L_{cr} (m)	5.13
W_y (cm^3)	4931.56
W_z (cm^3)	3928.35
N_{Ed} (KN)	11525.49

Table 10 - Length and axial force of element in design

5.3.1 Section Class
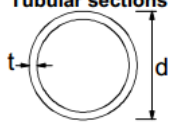
Figure 5-7 - Maximum ratios between the diameter and thickness (EN1993-1-1)

$$\frac{d}{t} = \frac{602}{16} = 37,63 \leq 70 * 0,66 = 46,2 \tag{23}$$

As the ratio between the diameter and the tickness is smaller than the limit of the class 2, the cross section resistance will be based on a plastic design.

5.3.2 Buckling resistance of members

In this part the stability of the member will be analysed doe to the effect of the buckling factor that will reduce the capacity of the section to support the axial force. As explained before, will be used the part 6.3.1.2 of the EN1993-1-1. The buckling curve used will be the "a", with a correspondent value of 0.21. The difference in this part is that the reducing factor will be calculated for both directions, once they have different inertias. In the first step is necessary to calculate the critical load and the respective slenderness to each direction.

$$N_{cr,y} = \frac{\pi^2 * E_t * I}{L_e^2} = \quad 134059,9 \; KN \tag{24}$$

$$N_{cr,z} = \frac{\pi^2 * E_t * I}{L_e^2} = \quad 92123,76 \; KN \tag{25}$$

$$\overline{\lambda_y} = \sqrt{\frac{A_g * f_y}{N_{cr}}} = \quad 0,304 \tag{26}$$

$$\overline{\lambda_z} = \sqrt{\frac{A_g * f_y}{N_{cr}}} = \quad 0,366 \tag{27}$$

$$\Phi_y = 0,5 * \left[1 + \alpha * (\overline{\lambda} - 0,2) + \overline{\lambda}^2\right] = \; 0,5570 \tag{28}$$

$$\Phi_z = 0,5 * \left[1 + \alpha * (\overline{\lambda} - 0,2) + \overline{\lambda}^2\right] = \; 0,5846 \tag{29}$$

With all the parameters needed calculated, is now possible to know the buckling factor for both the directions.

$$\chi_y = \frac{1}{\Phi + \sqrt{\Phi^2 - \overline{\lambda}^2}} = \quad 0,9766 \tag{30}$$

$$\chi_z = \frac{1}{\Phi + \sqrt{\Phi^2 - \overline{\lambda}^2}} = \quad 0,9614 \tag{31}$$

As the buckling factor in the z direction is smaller, is this one that will influence the design of the member, and will be applied to know the reduced axial capacity of the member.

$$N_{b,Rd} = \frac{\chi * A_g * f_y}{\gamma_{M1}} = \quad 11892,69 \; KN \tag{32}$$

Once this member is not subjected to bending moment, the verification is made comparing the axial force applied to the member and the reduced resistance of the member. With that in mind, the following expression gives us the result of the verification.

$$\frac{N_{Ed}}{N_{b,Rd}} = \frac{11525,49}{11892,69} = 0,969 \tag{33}$$

As shown in the formula above, the ratio of this element when verified to the buckling analysis is about 0.97, and, once is smaller than one, demonstrates that this element is well dimensioned, and have the appropriate properties, once the utilization is close to 100%. In this element the effect of the buckling in not very notorious, once the reduction factor only reduces the cross section resistance to axial compression force in about 4%.

5.3.3 Tension Verification

$$\sigma = \frac{N}{A} + \frac{M_{y,Ed}}{W_{pl,y}} + \frac{M_{z,Ed}}{W_{pl,z}} = \quad 330,7645 \quad MPa \tag{34}$$

Once the steel grade choose has a limit tension of 355 MPa, this cross section verifies this limit. Since the effect of the buckling is not from the major importance in this member, is possible to achieve higher tension in the cross sections.

5.4 Comparison of the solutions

Following the same dimensioning process presented before for all the elements in the structures, it's possible to compare and know what is the best solution for this type of hybrid tower. The weight of the structure is one of the most important factors, because it will have a direct influence on the price, but also the average utilization ratio is important to be compared, to get a real knowledge about the suitability of the cross sections in the different elements. On Table 11 are presented the results of both structures.

Geometry	Total Weight (Kg)	Maximum Ratio	Average Ratio
G_6_3	270640	0.97	0.83
G_8_2	272541	0.97	0.80

Table 11 - Results comparison of the solutions

Analysing all the data and results, it's possible to conclude that the structure with six supports its lighter, by a small margin, and has a higher average ratio of the sections. This are the favourable aspects of the six supported structure. One of the cons of this type of structure when compared to the eight supported one it's the higher number of different cross sections. When in the eight supported structure all the bars are more generic, and one cross section can be used in various elements without decreasing the average ratio, in the six supported the

same doesn't happen. Once the cross sections are made by bending plates, the more cross section used in the structure, more difficult it is to the industry to manufacture different cross sections. In the eight supported structure, the difficult to maintain the sections in the plastic limit, the class 1 or 2 of the cross section, is a major problem that decreases the average ratio of the utilization.

 With all the factors in mind, it's not clear what is the best solution, however, with the smaller weight, the six supported structure takes advantage when compared to the eight one. With the analysis of the connections, it will be easier to choose the best one. In the next chapter, that will be the focus of the study.

6 CONNECTION STUDY AND DESIGN

In this chapter, the connection between the different members of the lattice structure will be presented and designed, and the results of the two structures will be compared in order to get the best solution for this type of hybrid tower. Not only the number of bolts, but also the complexity of the connection, the way it affects the structure and the pre-work that has to be done to the cross section, as the holes to fit the bolts, are also parameters to have in account, due to the fact that it will influence the cost of the structure.

As stated before, the cross section consists in separate parts that are bolted together, in order to work as a circular cross section, and, this way, to easily the process of transportation and assembly in-situ. The way that makes this two processes easier, the reduction in connection costs, the gain of the fatigue design limitations when compared to the welding process, and the free maintenance of the connections, due to the use of pre-stressed bolts, are the main goals in using this type of cross section.

6.1 Type and class of the connection

A Structural link is a dispositive composed by different components, such as welds, bolts, plates, rivets, etc., that assure the continuity and transmission of efforts across the whole structure. In the case of the hybrid-towers in study, the disposal of the different elements leads to a K-type link, s represented in the part 7.1.2 of the EN1993-1-8. This type of connection in the structure in study is maintained by the gusset plates, that provide the area needed to connect the principal elements, chords, to the diagonal and horizontal elements.
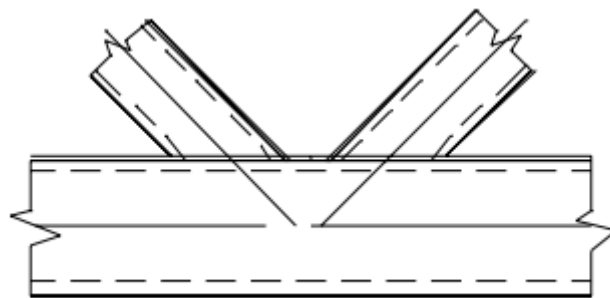
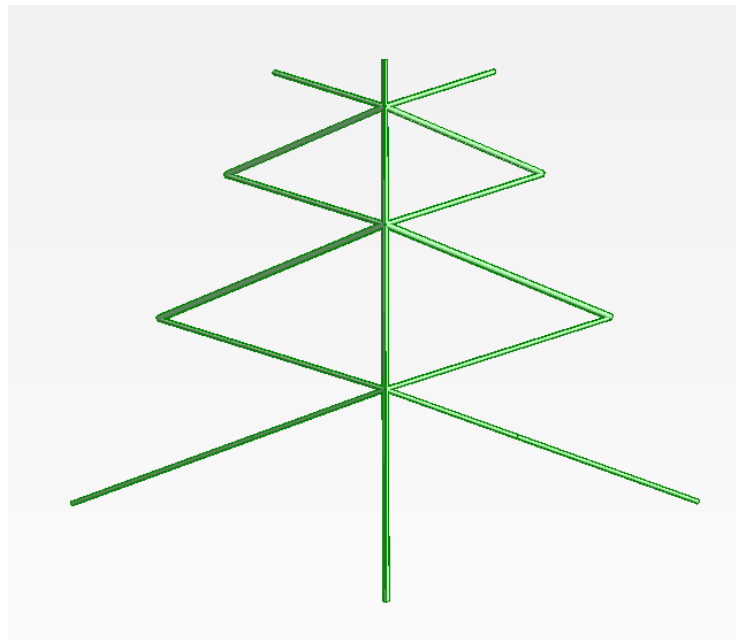Figure 6-1 - Representation of the K-joint according to the EN1993-1-8

Figure 6-2 - K connections in the case of study

With the purpose to maintain the connection in a free maintenance state, in the connections will be used pre-stressed bolts, which classifies the connection as a class C, where the slip resistance has to be verified for the ultimate resistance state. For this type of connections, the bolts used have to belong to the 8.8 or 10.9 class. Besides the slip resistance, the shear resistance per shear plane, and the bearing resistance of the gusset plates and the cross section will also be verified. In addition, for a connection in tension, the design plastic resistance of the net cross section at bolt holes, has to assure the support of the axial force that the element is subjected, in the ultimate limit state. In this particular case, the forces applied on the transverse direction of the cross section, y and z directions, can be dismissed, because the residual value that they represent, whereby the tension resistance of the bolts will not be verified. However, the bolts that will keep the different parts of the cross section together, will provide the sufficient support along the element, not only to maintain the characteristics of the cross section, but also to support this forces.

C slip-resistant at ultimate	$F_{v,Ed}$ $\leq$ $F_{s,Rd}$ $F_{v,Ed}$ $\leq$ $F_{b,Rd}$ $F_{v,Ed}$ $\leq$ $N_{net,Rd}$	Preloaded 8.8 or 10.9 bolts should be used. For slip resistance at ultimate see 3.9. $N_{net,Rd}$ see 3.4.1(1) c).

Figure 6-3 - Verifications needed for the C class connections

Once the diagonal and horizontal bars were modulated in the software as pinned in both ends, the connections designed forward will have no bending moment applied, and the bolts will only be subjected to shear efforts. The dimensioning rules applied in this chapter will be according to the EN1993-1-8, more specific, the part 3, who gives the rules for bolted

João Rafael Branquinho Maximino   46

connections. The material used for the gusset plates will be the S355 JR, and the bolts used will be from the 10.9 class, with a diameter of 20 or 30 mm, according to the total axial force that the connection needs to support, and in order to use the less amount of bolt in the whole structure.

6.2 Connection Design

In this part of the thesis, a numerical analysis will be perform in order to properly design the connections of both towers. Only one element will be analysed in the thesis, however all the connections were designed by the rules of the code stated before. In order to choose for which elements the connection should be studied, each level of the structure was analysed, and the nodes that connect elements with higher forces were selected and designed. For this case, the element analysed belongs to the six supported structure, and corresponds to a horizontal bar from the 3rd level, at 32 meters high, with a total length of 17.55 meters, the Sb cross section, and the axial force represented on Figure 6-5.
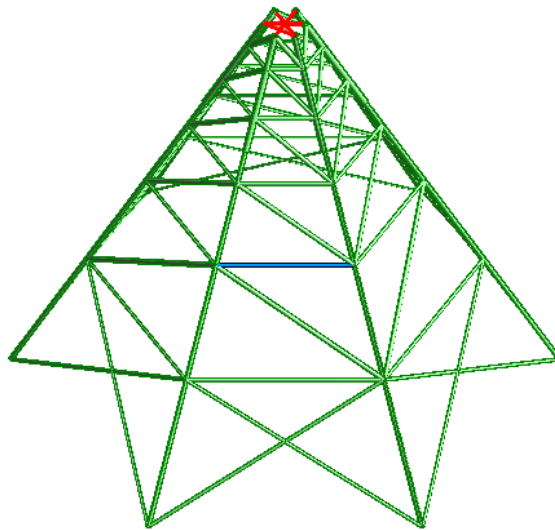

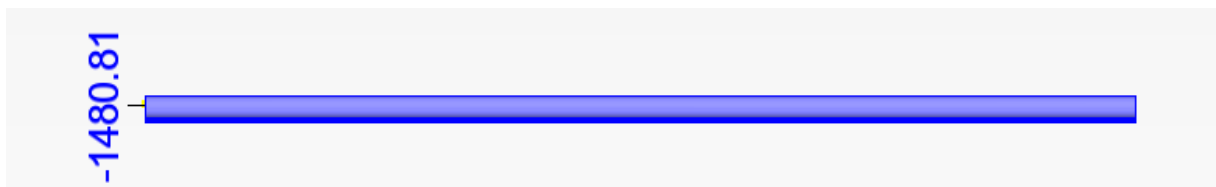Figure 6-4 - Element position on the structure - represented in blue

Figure 6-5 - Axial Force on the element in study

To verify the slip resistance, the section 3.9.1 of the EN1993-1-8 shows the formula needed to assure the right design. As so, the design slip resistance of one preloaded bolt can be calculated as shown in the following formulas.

$$F_{s,Rd} = \frac{k_s * n * \mu}{\gamma_{M3}} * F_{p,C} = \frac{1 * 2 * 0,5}{1,25} * 171,5 = 137,2 \, KN \tag{35}$$

$$F_{p,C} = 0,7 * f_{ub} * A_s = 0,7 * 1000^{-3} * 245 = 171,5 \, KN \tag{36}$$

Being the Ks a parameter related to the holes, n in the number of friction faces, μ is the slip factor, depending on the material, and A_s the net area of a M20 bolt, of the 10.9 class of resistance. With the resistance of one bolt calculated, is now possible to achieve the total amount of bolts needed for this connection.

$$\frac{N_{Ed}}{F_{s,Rd}} = \frac{1480,81}{137,2} = 12 \tag{37}$$

So, in this connection, in order to verify the slip resistance, there will be needed 12 M20 preloaded bolts.

In the next step, the shear resistance per shear plane of the bolts is verified, according to the formula presented on Table 3.4 of the EN 1993-1-8. As in our case, the shear planes appear in the threaded part of the bolt, the area to consider is the net area of the bolt.

$$F_{v,Rd} = \frac{\alpha_v * f_{ub} * A_s}{\gamma_{M2}} = \frac{0,5 * 1000^{-3} * 245}{1,25} = 98 \, KN \tag{38}$$

In this case, there are two shear planes in each bolt, and because of that, the shear resistance for each bolt is multiplied by two. Comparing the total of the axial force with the resistance of each bolt, we get the number of bolts needed for this verification.

$$\frac{N_{Ed}}{F_{v,Rd}} = \frac{1480,81}{2 * 98} = 8 \tag{39}$$

In the following step, the bearing resistance of the flange will be verified. The plate will not be calculated because it has a higher thickness when compared to the flange of the cross section, which makes this part the most critical one. For this analysis, several distances have to be established, as it is shown on Figure 6-6. The table 3.4 of the EN 1993-1-8 shows the formula to this verification.
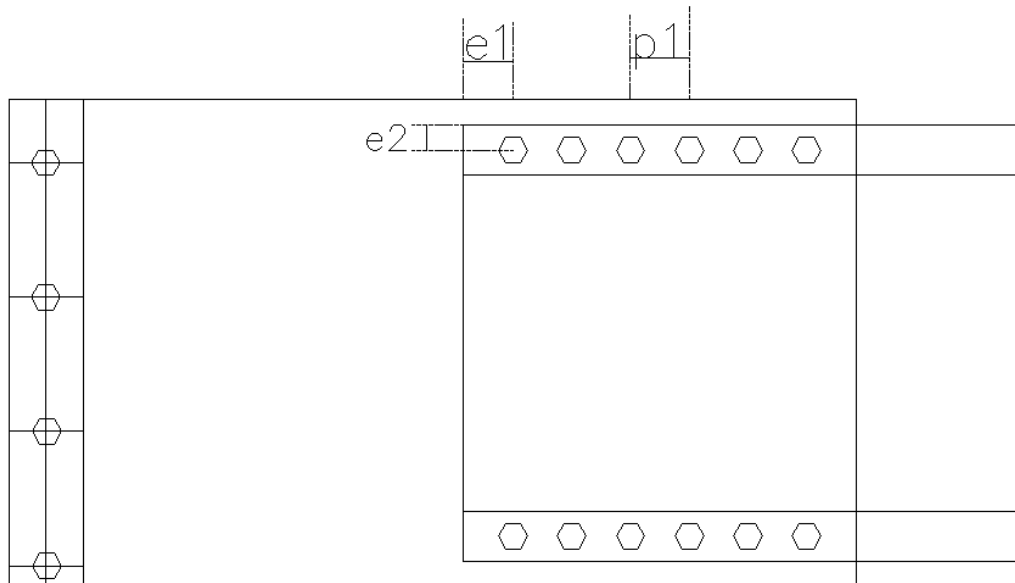
Figure 6-6 – Position of the bolts on the element

e_1 (mm)	60
e_2 (mm)	30
p_1 (mm)	70
d_0 (mm)	22
t (mm)	10

Table 12 - Distances on the connection

$$F_{b,Rd} = \frac{k_1 * \alpha_b * f_u * d * t}{\gamma_{M2}} \tag{40}$$

Where α_d is the smallest of α_b; f_{ub}/f_u and 1.To get the value of α_b on the direction of load transfer, it's necessary to compare the value of the end bolts and inner bolts.

$$\alpha_d = \frac{e_1}{3d_0} = 0,91 \; and \; \alpha_d = \frac{p_1}{3d_0} - \frac{1}{4} = 0,81 \tag{41}$$

$$\alpha_d = \min(0,81; 0,49; 1) = 0,49 \tag{42}$$

To analyse the perpendicular direction of the load, the K_1 parameter is needed. In the case in study, there are none inner bolts, so that, the only values to compare is between the minimum shown next.

$$k_1 = \min\left(2,8 * \frac{e_2}{d_0} - 1,7; 2,5\right) = 2,12 \tag{43}$$

With all the parameters determined, it's now possible to calculate the resistance of a hole when subjected to a load.

$$F_{b,Rd} = \frac{k_1 * \alpha_b * f_u * d * t}{\gamma_{M2}} = 81,4 \ KN \tag{44}$$

All that's left is to compare the resistance value with the real value. As we are analysing a flange, the value that the element is supporting has to be divided by 4, once we have 4 flanges on the cross section. By that, the total number of bolts needed to assure the behaviour of this verification is calculated in the following way.

$$\frac{N_{Ed}}{F_{b,Rd}} = \frac{1480,81/4}{81,4} = 5 \tag{45}$$

With all the verifications made, it's possible now to check the critical criteria of the connection. With the number of the bolts, it's possible to have a first idea of what is going to be. By that, and needing 12 bolts, the slip resistance is the most critical. This is to say that it's the one with the resistance more close to the applied value.

Design Criteria	Resistance Forces (KN)
Slip Resistance	**12*137.2=1646.4**
Shear Plane	12*(2*98)=2352
Bearing Resistance	12*81.4*4=3907.2

Table 13 - Critical Design Criteria

With the cross section verified, it's possible to design the plate that will maintain the elements together. In order to that, it's necessary to obtain the efforts from the other bar that connects in this node. The connection will be shown on Figure 6-7, as well as the efforts from each element.
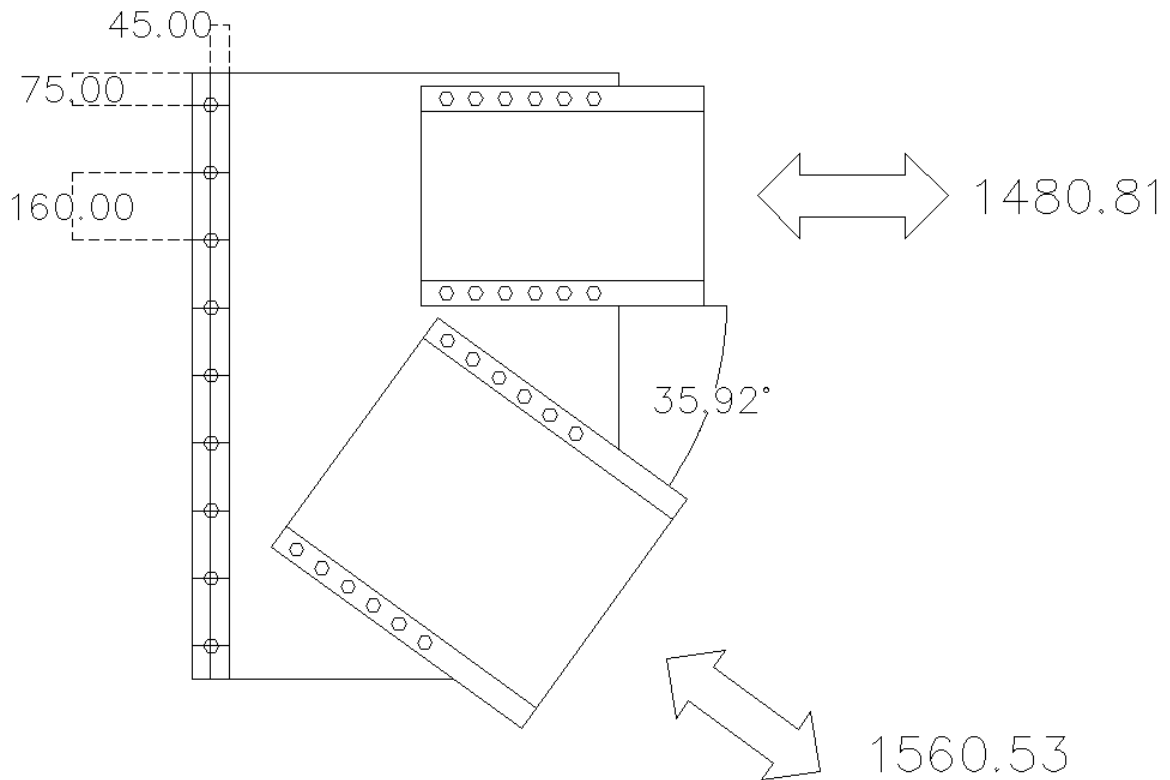
Figure 6-7 - Node Representation with the different elements

e_1 (mm)	75
e_2 (mm)	45
p_1 (mm)	160
d_0 (mm)	22
t_p (mm)	20
t_f (mm)	12.5
h_p (mm)	1433

Table 14 - Distances on the connection

In this case, it's also necessary to verify the connection on the slip resistance, the bearing resistance, the shear resistance of the bolts, and also, the capability of the plate to support the effort that is submitted. As that, in first place will be verified the slip resistance of the connection between the plate and the chord element. In order to get the design load, the vertical component of the diagonal force has to be obtained, because it's the force that is going to be transmitted as shear force for this connection, affecting this way the behaviour of the part in study. With this, this resultant force is equal to 915.5 KN.

$$N_{Ed,shear} = 1560,53 * sen(35,92) = 915,5 \ KN \tag{46}$$

Following the same steps as presented before, to calculate the resistance of one bolt, the next formulas are used.

$$F_{s,Rd} = \frac{k_s * n * \mu}{\gamma_{M3}} * F_{p,C} = \frac{1 * 2 * 0,5}{1,25} * 171,5 = 137,2 \ KN \qquad (47)$$

$$F_{p,C} = 0,7 * f_{ub} * A_s = 0,7 * 1000^{-3} * 245 = 171,5 \ KN \qquad (48)$$

$$\frac{N_{Ed}}{F_{s,Rd}} = \frac{915,5}{137,2} = 7 \qquad (49)$$

As this effort is transmitted as shear force, the bolts also have to be verified to the shear effect. The shear resistance is obtained according to the bolt used, in this case is also used the M20 bolt. In this case, there are also two shear planes per bolt, which gives the double resistance to each bolt. Having this into account, the verification comes in the following way.

$$F_{v,Rd} = \frac{\alpha_v * f_{ub} * A_s}{\gamma_{M2}} = \frac{0,5 * 1000^{-3} * 245}{1,25} = 98 \ KN \qquad (50)$$

$$\frac{N_{Ed}}{F_{v,Rd}} = \frac{915,5}{2 * 98} = 6 \qquad (51)$$

It's necessary to confirm the bearing resistance of the plate and the cross section that defines the chord of the structure. In this case, as the thickness of the cross section is smaller than the gusset plate, it's the one that is going to be dispensed attention in the analysis. The formula needed is presented as the equation (40) of this thesis. The parameters have to be calculated again, now for the values presented on Table 14. In the K_1 parameter, there are none inner bolts for this connection. As so, the comparison will be made only for the end bolts and the minimum value of 2,5. In this case, as we have two flanges connected to the gusset plate, the value to compare is only half of the applied, because it will be divided by the two portions that make the cross section.

$$\alpha_d = \frac{e_1}{3d_0} = 1,14 \ and \ \alpha_d = \frac{p_1}{3d_0} - \frac{1}{4} = 2,17 \qquad (52)$$

$$\alpha_d = \min(1,14; 0,49; 1) = 0,49 \qquad (53)$$

$$k_1 = \min\left(2,8 * \frac{e_2}{d_0} - 1,7; 2,5\right) = 2,5 \qquad (54)$$

$$F_{b,Rd} = \frac{k_1 * \alpha_b * f_u * d * t}{\gamma_{M2}} = 120,05 \ KN \qquad (55)$$

$$\frac{N_{Ed}}{F_{b,Rd}} = \frac{915,5/2}{120,05} = 4 \tag{56}$$

As it's possible to conclude from the analysis made, 7 bolts would be enough to assure the right continuity and distribution of forces. However, the EN 1993-1-8 limit the distance between bolts in 200 mm. In order to fulfil that requirement in our connection, the total number of bolts had to be increased to 9 bolts, as represented on Figure 6-7.

Design Criteria	Resistance Forces (KN)
Slip Resistance	**9*137.2=1234.8**
Shear Plane	9*(2*98)=1764
Bearing Resistance	9*120.05*2=2160.9

Table 15 - Critical Design Criteria

The vertical resultant of the two elements is verified. On the other hand, the horizontal force is yet to be verified. This component will be supported by the area of the gusset plate that holds the two elements together. This area is obtained by the total height of the gusset plate, subtracted by the dimension of the holes, in this case 9 holes with a diameter of 22 mm. The total horizontal effort is calculated by the formula (57).

$$N_{Ed} = 1480,81 + 1560,53 * \cos(35,92) = 2744,59 \, KN \tag{57}$$

$$A = (1433 - 9 * 22) * 20 = 24700 \, mm^2 \tag{58}$$

$$N_{Rd} = \frac{A * f_y}{\gamma_{M0}} = \frac{24700 * 355 * 10^{-3}}{1} = 8768,5 \, KN \tag{59}$$

$$\frac{N_{Ed}}{N_{Rd}} = \frac{2744,59}{8768,5} = 0,32 < 1 \tag{60}$$

The only verification left, has to do with the cross section area without the holes. As it is an element in tension, the net cross section has to be verified for the force applied on the element. In this way, the net area of the element and the resistance axial force are equal to:

$$A_{net} = 14468 - 4 * 22 * 10 = 13588 \, mm^2 \tag{61}$$

$$N_{Rd} = 13588 * 355 * 10^{-3} = 4755,8 \, KN \tag{62}$$

$$\frac{N_{Ed}}{N_{Rd}} = \frac{1480,81}{4755,8} = 0,31 < 1 \tag{63}$$

6.3 Comparison of the solutions

With the same procedure followed before, and all the connections of both structures designed, it's possible to make a more complete study on the complexity, the amount of materials and time needed to assemble the lattice structure. The total number of bolts needed for the connections for each structure will be presented, and an approximate value for the bolts needed to complete the cross sections will be calculated using the total length of the elements, in order to compare the results.

Geometry	Bolts in connections (M20)	Bolts in connections (M30)	Bolts in cross sections	Total
G_6_3	1812	1062	4120	6994
G_8_2	3304	800	4610	8714

Table 16 - Total amount of bolts needed for each structure

Previously, on this thesis, the comparison of both structures with the results of total weight and average utilization of the elements didn't give a clear difference between the two structures. However, with the results of the materials needed for the connections, it's easy to conclude that the structure with six supports uses much less material, has less connections, and the complexity of these connections are simpler. In the amount of bolts needed, the difference is about 20% less on the six supported structure, which also leads to a cost-saving in time of assembly.

7 Conclusions

Once the total height of the towers was limited by the transportation issues, new solutions are needed in order to achieve better results and a higher performance for the wind energy. With this thesis, it was proved that a hybrid solution made from a lattice part and a tubular tower is a good alternative to overcome this limitation.

With the type of cross section used in this study, the transportation issue is overcome, once it's possible to transport the lattice structure in individual parts to the construction site, and then to assemble the structure in a short space of time, and using only bolted connections. However, the difficulty to keep the cross sections in a class were the plastic properties off the steel could contribute to a better solution were the main obstacle in the dimensioning and verification process.

During the assembly of the lattice tower, one of the laterals of the structure is free of diagonal and horizontal elements until 28 meters in the eight supported structure, and 32 meters on the six supported one, in order to make the process of erecting the tubular structure easier. This situation has been taken into account on the dimensioning process, with all the verifications made for this specific situation. Nevertheless, when the assembly of the structure is being made, for safety and work conditions, the wind speed is not the same as if the tower was in full function, but a lower one. With that, and being the verification made for the condition of extreme wind situation, the design of the tower without the elements mentioned before is secured.

As showed on Table 11 and Table 16, the lattice tower with six supports is the best and most reliable alternative for this hybrid structures. Not only needed the less amount of steel, but mostly to the minor and less complex number of connections and connecting elements, such as bolts, the holes on the cross sections and plates, and gusset plates. This will lead to a more economic structure, not only on the materials, but also in the hand work to assembly the structure.

8 References

Corbetta, G. (2014), EWEA – "The European offshore Wind Industries – Key trends and statistics 2013"

EN 1991-1-1:2009, "Eurocode 1 – Actions on structures – Part 1-1: General actions densities, self-weight, imposed loads for buildings", European Committee for Standardization, 2009.

EN 1993-1-1:2010, "Eurocode 3 – Design of steel structures – Part 1-1: General rules and rules for buildings", European Committee for Standardization, 2010.

EN 1993-1-5:2010, "Eurocode 3 – Design of steel structures – Part 1-3 General rules - Supplementary rules for cold-formed members and sheeting", European Committee for Standardization, 2010

EN 1993-1-5:2010, "Eurocode 3 – Design of steel structures – Part 1-5: Plated structural elements", European Committee for Standardization, 2010

EN 1993-1-5:2010, "Eurocode 3 – Design of steel structures – Part 1-6: Strength and Stability of Shell Structures", European Committee for Standardization, 2010

EN 1993-1-8:2010, "Eurocode 3 - Design of steel structures - Part 1-8: Design of joints", European Committee for Standardization, 2010

EN 1993-1-9:2010, "Eurocode 3 – Design of steel structures – Part 1-9: Fatigue", European Committee for Standardization, 2010

EWEA (2015) – "Wind in Power – 2014 European Statistics"

Freid, L. (2015), GWEC – "Global Wind Statistics 2014"

Garzon, O. (2013), "Resistance of Polygonal cross-sections – Application on steel towers for wind turbines". Licentiate thesis, Department of civil, environmental and natural resources engineering, Lulea University of Technology.

Hau, E. (2013), "Wind Turbines – Fundamentals, Technologies, Applications, Economics", Springer, Munich

Jan van der Tempel (2006). "Design of support structures for offshore wind turbines". PhD Thesis, Delft University of Technology, Netherlands.

Kubiak, T. (2013), "Static and Dynamic Buckling of Thin-Walled Plate Structures", Springer, London

LaNier, M.W. (2005) "LWST Phase I – Project Conceptual Design Study: Evaluation of Design and Construction Approaches for Economical Hybrid Steel/Concrete Wind Turbine Towers", NREL, Colorado

Martins, J. P., Simões da Silva, L., Reis, A. (2013) "Eigenvalue analysis of cylindrically curved panels under compressive stresses – Extension of rules from EN1993-1-5". Thin-Walled Structures, vol 69, pg 183-194

Martins, J. P., Simões da Silva, L., Reis, A. (2014) "Ultimate load of cylindrically curved panels under in-plane compression and bending – Extension of rules from EN1993-1-5". Thin-Walled Structures, vol 77, pg 36-47

Rebelo, C., Simões da Silva L. (2012) "Foundation concepts for ofsshore wind farms", Institute for Sustainability and Innovation In Structural Engineering (ISISE). University of Coimbra.

Rebelo,C. , Moura,A. , Gervásio,H. , Veljkovic,M. ,Simões da Silva, L. "Comparative life cycle assessment of tubular wind towers and foundations – Part 1: Structural Design". Engineering Structures, Vol 74, pg 283-291

Simões, R.A.D. (2014), "Manual de Dimensionamento de Estruturas Metálicas", CMM, Coimbra

Spera, D. (2012), "Wind Turbine Technology – Fundamental Concepts of Wind Turbine Engineering", ASME, New York

Stowell, E. (1943) "Critical compressive stress for curved sheet supported along all edges and elastically restrained against rotation along the unloaded edges". National Advisory Committee for Aeronautics, NACA, Washington

Tran, Anh Tuan (2014), "Resistance of circular and polygonal steel towers for wind turbines". Licentiate thesis, Department of civil, environmental and natural resources engineering, Lulea University of Technology.

Veljkovic, M. et al (2012), "High Strength Tower in Steel for Wind Turbines – HISTWIN", Research Final Report

Winterstetter, Th.A., Schmidt, H. (2002) "Stability of circular cylindrical steel shells under combined loading". Thin-Walled Structures, vol 40, pg 893-909

Annex

Buckling Resistance for Elements

$N_{Ed} =$ 13007,51 KN Axial Force

$M_{y,Ed} =$ 92,68 $KN.m$ Bending Moment Direction y

$M_{z,Ed} =$ 674,32 $KN.m$ Bending Moment Direction z

$\gamma_{M1} =$ 1

$f_y =$ 355 MPa Yield Strenght

$E =$ 210 GPa Modulus of Elasticity

$L_{cr} =$ 4470 mm Lenght of the member

$A_g =$ 518,47 cm^2 Area of cross section

$I_y =$ 387087,86 cm^4 Moment of Inertia Direction y

$I_z =$ 360723,4 cm^4 Moment of Inertia Direction z

$\alpha =$ 0,21   Imperfection Factor EN 1993-1-1 (Table 6.1)

$W_{pl,y} =$ 8890,85 cm^3 Plasticity Modulus Direction y

$W_{pl,z} =$ 7883,56 cm^3 Plasticity Modulus Direction z

Buckling Resistance of Members
Uniform members in compression

$$N_{b,Rd} = \frac{\chi * A_g * f_y}{\gamma_{M1}} = \quad 18317,56 \ KN$$
Design Buckling resistance of a compression member
EN 1993-1-1 (6.3.1)

$$\chi_y = \frac{1}{\Phi + \sqrt{\Phi^2 - \bar{\lambda}^2}} = \quad 0,9969$$
Buckling reduction factor - Direction y
EN1993-1-1 (6.49)

$$\Phi_y = 0,5 * \left[1 + \alpha * (\bar{\lambda} - 0,2) + \bar{\lambda}^2\right] = \quad 0,5244$$
EN1993-1-1 (6.49)

$$\chi_z = \frac{1}{\Phi + \sqrt{\Phi^2 - \bar{\lambda}^2}} = \quad 0,9952$$
Buckling reduction factor - Direction z
EN1993-1-1 (6.49)

$$\Phi_z = 0,5 * \left[1 + \alpha * (\bar{\lambda} - 0,2) + \bar{\lambda}^2\right] = \quad 0,5269$$
EN1993-1-1 (6.49)

$$N_{cr,y} = \frac{\pi^2 * E_t * I}{L_e^2} = \quad 401525,9 \ KN$$
Elastic critical Force for the relevant critical mode

$$N_{cr,z} = \frac{\pi^2 * E_t * I}{L_e^2} = \quad 374178,1 \ KN$$
Elastic critical Force for the relevant critical mode

$$N_{Rk} = A_g * f_y = \quad 18405,69 \ KN$$

Buckling Resistance for Elements

$$\overline{\lambda_y} = \sqrt{\frac{A_g * f_y}{N_{cr}}} = \qquad 0{,}21$$

Non-dimensional Slenderness - Direction y
EN1993-1-1 (6.49)

$$\overline{\lambda_z} = \sqrt{\frac{A_g * f_y}{N_{cr}}} = \qquad 0{,}22$$

Non-dimensional Slenderness - Direction z
EN1993-1-1 (6.49)

Uniform members in bending

$$\chi_{LT} = \qquad 1$$

Reduction factor for lateral torsion buckling

$$M_{b,Rd,y} = \chi_{LT} * W_{pl,y} * \frac{f_y}{\gamma_{M1}} = \qquad 3156{,}252 \; KN$$

Buckling resistance moment y
EN 1993-1-1 (6.55)

$$M_{b,Rd,z} = \chi_{LT} * W_{pl,z} * \frac{f_y}{\gamma_{M1}} = \qquad 2798{,}664 \; KN$$

Buckling resistance moment z
EN 1993-1-1 (6.55)

Uniform members in bending and axial compression

Table B.3: Equivalent uniform moment factors Cm

$My_{,left}=$	0	$Mz_{,left}=$	0
$My_{,right}=$	92,68	$Mz_{,right}=$	674,32
$\varphi =$	0,00000	$\varphi =$	0,00000
$C_{my}=$	0,60000	$C_{mz}=$	0,60000

Method 2: Interaction factors k_{ij} for interaction formula in 6.3.3(4) - Table B.1 EN1993-1-1

$$k_{yy} = \qquad 0{,}6060 \qquad\qquad k_{zy} = \qquad 0{,}3636$$

$$k_{yz} = \qquad 0{,}3656 \qquad\qquad k_{zz} = \qquad 0{,}6093$$

Members which are subjected to combined bending and axial compression should satisfy the formulas (6.61) and (6.62) of EN 1993-1-1: 2005

$$\frac{N_{Ed}}{\dfrac{\chi_y N_{Rk}}{\gamma_{M1}}} + k_{yy} \frac{M_{y,Ed} + \Delta M_{y,Ed}}{\chi_{LT} \dfrac{M_{y,Rk}}{\gamma_{M1}}} + k_{yz} \frac{M_{z,Ed} + \Delta M_{z,Ed}}{\dfrac{M_{z,Rk}}{\gamma_{M1}}} = 0{,}814778$$

$$\frac{N_{Ed}}{\dfrac{\chi_z N_{Rk}}{\gamma_{M1}}} + k_{zy} \frac{M_{y,Ed} + \Delta M_{y,Ed}}{\chi_{LT} \dfrac{M_{y,Rk}}{\gamma_{M1}}} + k_{zz} \frac{M_{z,Ed} + \Delta M_{z,Ed}}{\dfrac{M_{z,Rk}}{\gamma_{M1}}} = 0{,}867587$$

Bending and Axial Force
Classification of Cross Section

$\varepsilon^2 =$ 0,66   Coefficient depending on f_y

$d =$ 737 mm Equivalent diameter of cross section

$t =$ 16 mm Thickness of the plate

$\dfrac{d}{t} =$ 46,06   Relation between diameter and thickness

$50 * \varepsilon^2 =$ 33   Class 1 limit relation

$70 * \varepsilon^2 =$ 46,2   Class 2 limit relation

$90 * \varepsilon^2 =$ 59,4   Class 3 limit relation
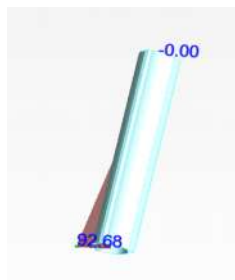
Bending and axial force verification

$M_{N,y,Rd} = M_{pl,y,Rd}(1 - n^{1,7}) =$ 1406,875   Axial reduced Bending Resistance Moment y
EN1993-1-1 (6.41)

$M_{N,z,Rd} = M_{pl,z,Rd}(1 - n^{1,7}) =$ 1247,483   Axial reduced Bending Resistance Moment z
EN1993-1-1 (6.41)

$n = \dfrac{N_{Ed}}{N_{pl,Rd}} =$ 0,70671   Reduced Axial Efford

$\left[\dfrac{M_{y,Ed}}{M_{N,y,Rd}}\right]^2 + \left[\dfrac{M_{z,Ed}}{M_{N,z,Rd}}\right]^2 =$ 0,2965   Bi-axial Bending Verification
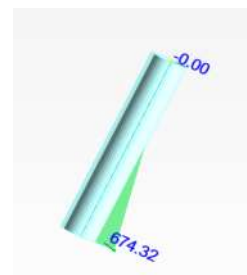EN1993-1-1 (6.41)

Tension Verification

$\sigma = \dfrac{N}{A} + \dfrac{M_{y,Ed}}{W_{pl,y}} + \dfrac{M_{z,Ed}}{W_{pl,z}} =$ 346,8418 MPa
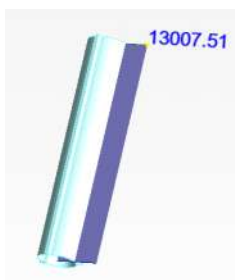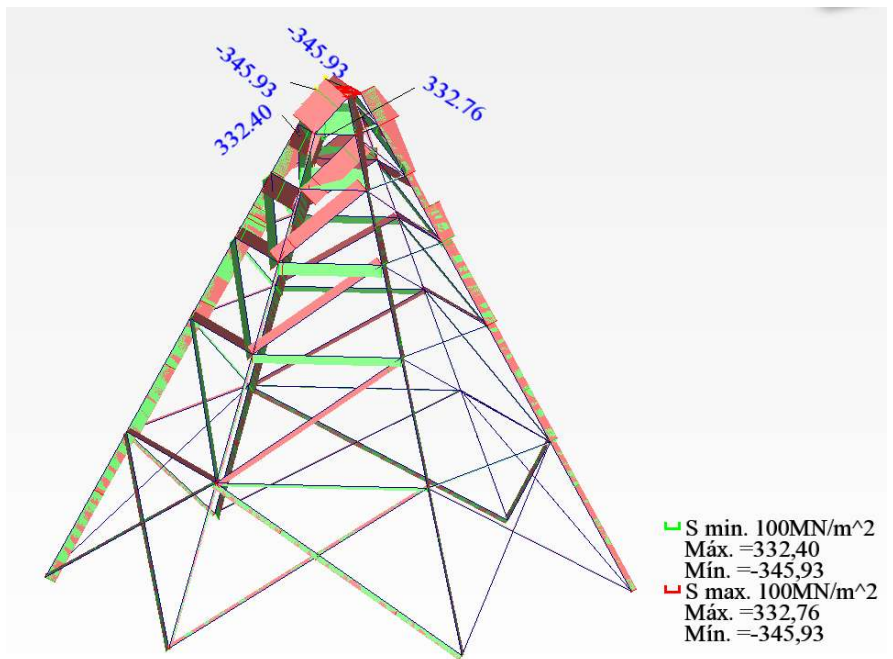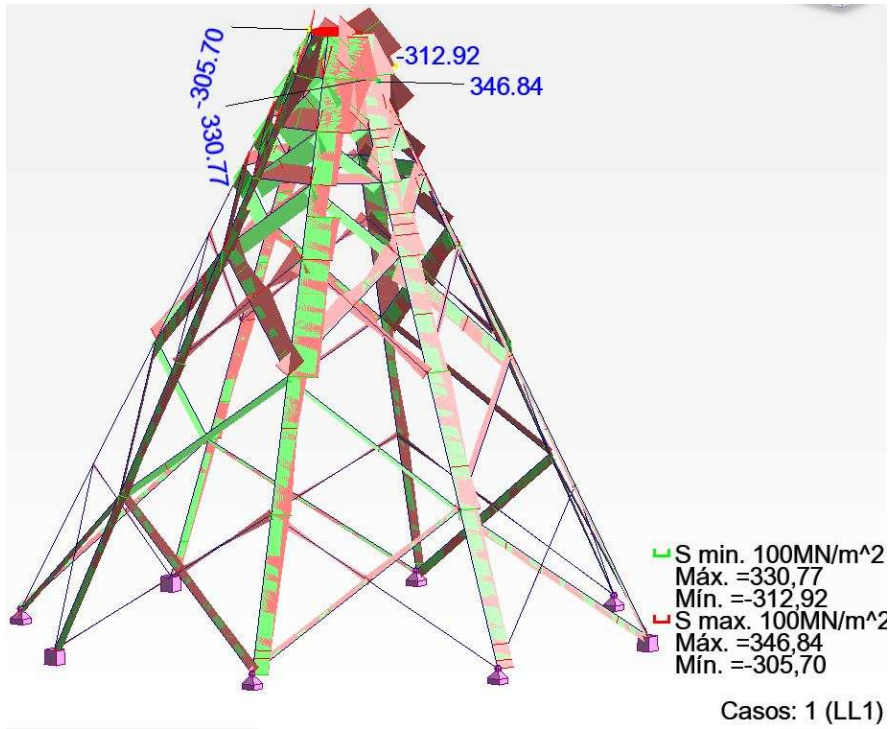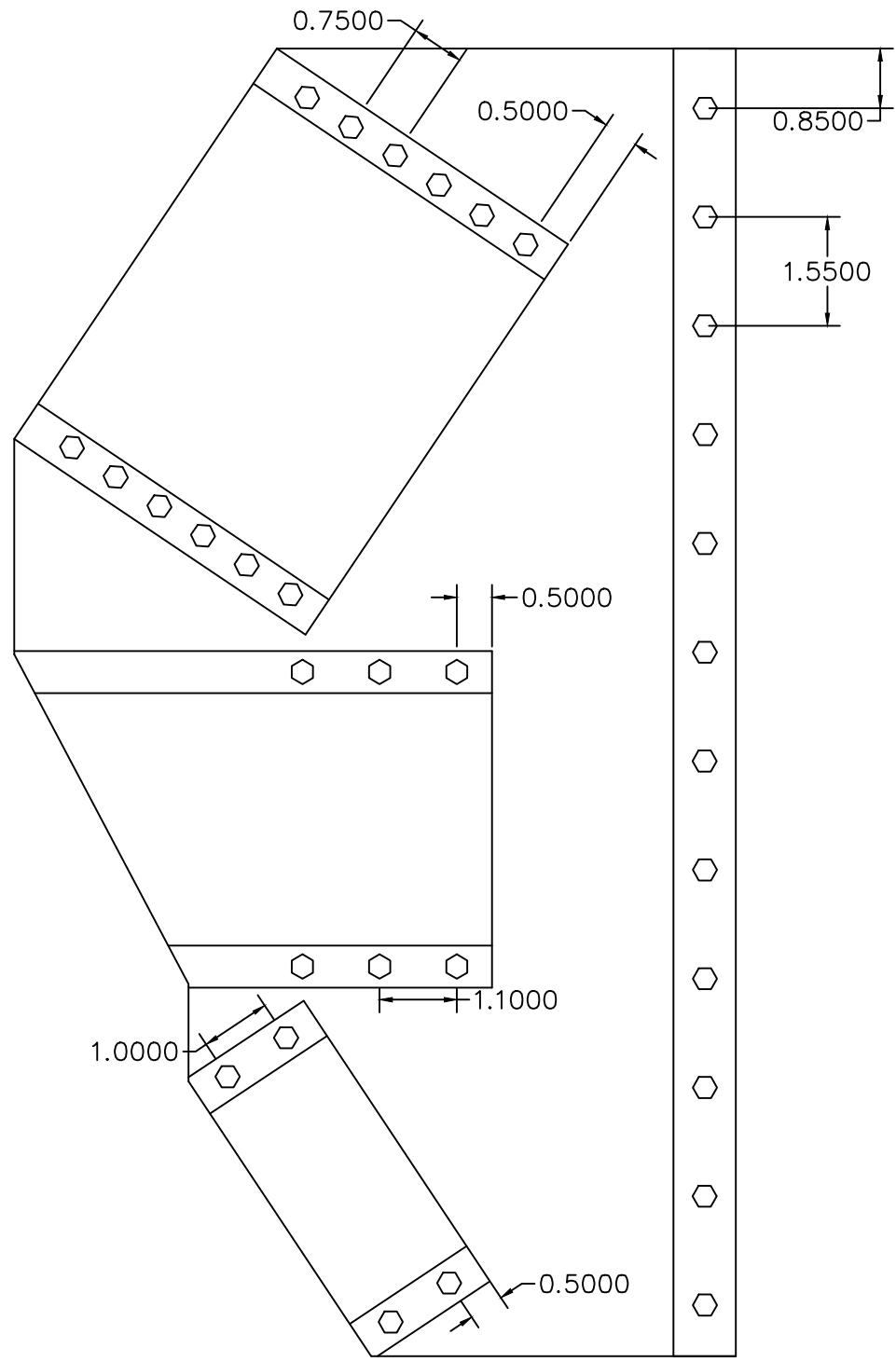

Axial Force - x Direction   Bending Moment - Y Direction   Bending Moment - Z Direction

Annex B – Maximum Stresses

0.7500

0.5000

0.8500

1.5500

0.5000

0.5000

1.1000

1.0000

	Julho 2015		
			João Maximino
Escala	1:10	**Departamento Engenharia Cívil** **Dissertação em Mecânica Estrutural**	
		Six Supported Structure Connection	